Divergent modulation of dopaminergic neurons by hypocretin/orexin receptors-1 and -2 shapes dopaminergic cell activity and socio-emotional behavior

Stamatina Tzanoulinou[1], Simone Astori[2], Laura Clara Grandi[3], Francesca Gullo[3], Richie Kalusivikako[1], Simran Rai[1], Mehdi Tafti[1], Andrea Becchetti[3], and Anne Vassalli[1] ✉

[1] *Department of Biomedical Sciences, University of Lausanne, Lausanne, Switzerland.*
[2] *Laboratory of Behavioral Genetics, EPFL, Switzerland.*
[3] *Department of Biotechnology and Biosciences and NeuroMI (Milan Center of Neuroscience), University of Milano-Bicocca, Milano, Italy.*

✉Corresponding author: anne.vassalli@unil.ch

Keywords: Dopamine, Hypocretin/Orexin, OX_1 receptor, OX_2 receptor, socioemotional behavior, anxiety, hyperactivity, impulsivity, compulsivity

This PDF file includes:

Main Text
Figures 1-7
Supplementary Information: Figures S1-S3
Table S1

ABSTRACT

Many neuropsychiatric disorders involve dysregulation of the dopaminergic (DA) input to the forebrain. Of particular relevance are DA projections originating from the midbrain ventral tegmental area (VTA). A key neuromodulatory influence onto DA^{VTA} neurons arises from the dense axonal projections emanating from lateral hypothalamic area hypocretin/orexin (OX) neurons. Despite being a major input, the differential action of orexin peptides A and B (OXA and OXB) on orexin receptors 1 and 2 (OX_1R and OX_2R) in DA cells is poorly characterized. We thus genetically engineered mice whose DA neurons are selectively unresponsive to OX input via OX_1R ($DA^{Ox1R\text{-}KO}$ mice) or OX_2R ($DA^{Ox2R\text{-}KO}$ mice) and compared their behavior and DA cell electrophysiology to genetic controls. We previously showed a profound functional divergence between OX_1R- and OX_2R-mediated modulation of DA neurons in controlling vigilance states, brain oscillations and cognitive behavior. Inactivation of OX_2R, but not OX_1R, in DA neurons dramatically increased time spent in EEG theta-rich wakefulness, improved reward-driven learning and attentional skills, while it impaired inhibitory control. Here, we interrogate $DA^{Ox1R\text{-}KO}$ and $DA^{Ox2R\text{-}KO}$ mice in further behavioral domains. We show that mice with DA-specific OX_1R loss exhibit hyperactivity, or anxiety-like responding, in context-dependent manners. OX_2R loss in contrast decreases sociability and aversion-driven learning. We next investigate the underlying electrophysiological substrates and uncover previously unrecognized effects of OX peptides on DA^{VTA} cell responses. In WT and control mice, we show that while OXA enhances, OXB diminishes DA^{VTA} neuronal excitability. OX_1R-deficient DA cells lose OXA responding and OX_2R-deficient DA cells lose OXB responding. We altogether evidence strikingly distinct functions of OX_1 vs OX_2R signaling in modulating the intrinsic excitability of DA^{VTA} neurons and influencing DA-related behaviors. Our data position OX→DA neurotransmission via OX_1 or OX_2R as relevant to endophenotypes observed in the context of disorders such as obsessive-compulsive, attention-deficit/hyperactivity, and autism spectrum disorders.

INTRODUCTION

Neuromodulators are small molecules released by neurons which act primarily through 'volume transmission' at both synaptic and extra-synaptic G-protein-coupled receptors. This broad range of action leads to modulation of cellular and synaptic properties of neurons across widespread brain areas, enabling profound reconfiguration of the output of neural circuits.

Noradrenaline (NA), dopamine (DA), serotonin (5-hydroxytryptamine, 5HT), histamine, acetylcholine, and the hypocretin/orexin (HCRT/OX) neuropeptides are the main molecules that can act as neuromodulators of wakefulness. The dopaminergic (DA) and HCRT/OX systems are also key hubs of the motivational network. Neurons of the HCRT/OX system release neuropeptides known as hypocretin-1 and -2[1], or orexin A and B (OXA and OXB)[2]. Following the official nomenclature for the gene encoding the precursor to both peptides, we will use *Hcrt* for genes, but OXA and OXB for the gene products. The population of hypothalamic glutamatergic cells that synthesize OXA and OXB is a central hub for arousal induction and maintenance. These neurons act as multi-modal sensors and integrators of incoming signals from the internal or external environments, which in turn broadcast effector signals throughout the brain by their extensive projections to all wake-promoting monoaminergic and cholinergic nuclei and to their targets in the neocortex, thalamus, hippocampus, amygdala and spinal cord[3].

OX cells fire maximally during active wakefulness, in line with their role in maintaining heightened arousal, but also show critical transient firing across non-rapid-eye-movement sleep (NREMS)[4] and phasic REMS[5]episodes, in line with their role in inducing sleep-to-wake transitions[6] and stabilizing behavioral states[7]. OX loss severely compromises the integrity and stability of the three cardinal vigilance states: wakefulness, NREMS and REMS[8,9]. OX deficit causes a lifelong debilitating disease, called narcolepsy type-1 (NT-1)[10].

OX activity is mediated by signaling elicited by two genetically independent and differentially expressed GPCRs, OX_1R and OX_2R, respectively encoded by the *Hcrtr1* and *Hcrtr2* genes. OX signaling is critically implicated in physiological and pathological processes as diverse as alertness modulation, energy metabolism, food intake, drug reward, autonomic and endocrine regulation, anxiety and depression-related behaviors. OXA binds both OX_1R and OX_2R with high affinity, whereas OXB has higher affinity for OX_2R[2,11]. Although genetic evidence in both dogs and mice points to a stronger involvement of OX_2R in vigilance state regulation, most studies have focused on OXA and OX_1R function, resulting in underexplored appreciation of the specific functions of OXB and OX_2R signaling. Hence, the brain levels of the two peptides and the differential signaling and role of the two receptors remain essentially unknown, despite their suspected implication in many disorders. OX neurons respond to salient stimuli of either negative or positive valence, across multiple metabolic and sensory modalities, and are implicated in both stress and reward-associated plasticity. Low glucose or O_2, changes in CO_2 or pH, visual, acoustic, olfactory stimuli, all activate OX neurons. Meanwhile, positive stimuli such as highly palatable food, emotional elation, social reunion can trigger cataplexy, the decoupling of wakefulness with motor tone, which is the quintessential pathognomonic symptom of NT-1 and signature of OX signaling deficiency[12].

OX neurons exert their effects through wide projections to the brain areas involved in arousal, motivation and stress-related responses, such as the basal forebrain, locus coeruleus (LC), dorsal raphe, extended amygdala, ventral tegmental area (VTA), *nucleus accumbens* (NAc) and medial prefrontal cortex

(mPFC)[3,13,14]. Many lines of evidence suggest that DA is a major effector of the OX system. For instance, daytime sleepiness and cataplexy are key symptoms of NT-1, whose physiological bases are fundamentally different. Nonetheless, both stem from OX deficiency, and both respond to dopaminergic drugs. In narcoleptic dogs and mice, sleep attacks respond to D1-receptor agonists, while cataplexy responds to D2/D3-receptor antagonists[15,16]. In general, the VTA dopaminergic neurons (DA^{VTA}) appear to stand at the root of the behavioral implications of the OX-DA interplay. Both VTA and NAc belong to the mesolimbic reward system, critically involved in reward processing and motivated behaviors, with DA^{VTA} projecting heavily to the medium spiny neurons of the NAc[17,18]. In turn, OX neurons densely project to DA^{VTA} neurons, which express both *Hcrtr1*/*Ox₁R* and *Hcrtr2*/*Ox₂R*[19]. However, the precise functional role of OX at the interface of the mesolimbic reward system[20-22] and the specific contribution of OX_1R and OX_2R to the modulation of reward and motivation are not fully solved.

From a cellular standpoint, OX stimulation elicits different firing patterns in different DA^{VTA} cell subsets, and single cells may express either *Hcrtr1*, *Hcrtr2*, or both receptors[23]. In general, the prevalent effect of OXA on DA^{VTA} cells appears to be excitatory, as OXA elevates $[Ca^{2+}]_{intracell}$ in isolated rat DA^{VTA} neurons[24], and enhances DA^{VTA} firing and induce tetrodotoxin-resistant depolarization in brain slices[23]. OX is thought to stimulate DA^{VTA} activity both by direct OXR activation on DA somatodendritic compartment, and indirectly by potentiating glutamatergic afferents[23,25,26]. In fact, Borgland *et al* showed that OXA potentiates N-methyl-D-aspartate receptor (NMDAR) transmission in DA^{VTA} synapses *ex vivo*, while OX_1R antagonism blocks locomotor sensitization to cocaine in mice *in vivo*, as well as occludes VTA AMPA/NMDA ratio increase *ex vivo*, a proxy for plasticity normally observed following cocaine exposure[25]. Borgland and collaborators later showed that optical stimulation of OX neuronal terminals in the VTA is insufficient by itself to alter DA release in the NAc[27]. However, when OX→DA optical stimulation is coupled with intra-VTA electrically-evoked stimulation, it markedly elevates DA levels in the NAc core, which is blocked by OX_1R antagonism[27]. OXA-mediated OX_1R signaling therefore appears to potentiate VTA→NAc dopaminergic transmission, presumably by recruiting VTA glutamatergic afferents.

The effect of OXB on DA^{VTA} neurons turned out to be even more complex, with some neurons responding to OXB exposure with alternate periods of silent hyperpolarization and firing, or a bursting firing mode[23]. The mechanisms underlying these different responses remain unsolved. Once again, they may result from the integration of both cell-autonomous (direct) effects of OXB on OXRs expressed on somato-dendritic membranes as well as indirect effects on OX receptors located on local GABAergic terminals that modulate DA neuronal activity.

To functionally interrogate orexinergic modulation of DA signaling in sleep/wake regulation and other DA-dependent behaviors, we previously generated mice whose *Hcrtr1* or *Hcrtr2* genes were selectively disrupted in DA neurons (respectively, $DA^{Ox1R\text{-}KO}$ and $DA^{Ox2R\text{-}KO}$). Inactivation of OX_2R signaling in dopaminergic neurons induces hyperarousal, enhanced EEG theta-gamma phase-amplitude coupling and improved cognition, but induces impulsive- and compulsive-like behavioral patterns[19]. Our genetically based mutants lacking OX_1 and/or OX_2R selectively in DA cells also allow to parse out the different contributions of the two receptors to DA^{VTA} cell physiology. In the present paper, we present the main behavioral alterations caused by *Hcrtr1* or *Hcrtr2* deletion in DA cells, in the light of the physiological effects of OX stimulation of DA^{VTA} neurons, studied at the cellular level. Besides expanding fundamental knowledge, distinguishing the role of either receptor in different behavioral tasks is likely to have

significant pharmacological implications in psychiatry. Moreover, targeting individual OX receptors in a clinical setting may be planned considering their differential effects on the sleep-waking cycle. Blocking OX_2R reduces wakefulness, whereas selectively antagonizing OX_1R may allow to achieve clinical efficacy without promoting sleep[28].

RESULTS

Divergent effects of OXA and OXB peptides in dissociated DA^{VTA} neurons of WT mice.

Shortly after the discovery of hypocretin/orexin peptides, a study by Korotkova and colleagues revealed that application of OXA on rat VTA slices increases the spontaneous firing rate of DA neurons, while the effect of OXB was more heterogeneous and included phasic firing effects[23]. To further characterize how OX peptides modulate the activity of DA neurons and assess the kinetic features of DA neuronal response, we first collected data from dissociated single neurons to exclude confounding synaptic effects implicating other cell types. As DA cells from the VTA were the first to be shown to respond to OX peptides, and *substantia nigra* DA neurons were shown not to respond[29], we performed patch-clamp recordings of DA cells acutely dissociated from VTA slices of 2-3-week old mice (see criteria for DA cell identification in Materials and Methods). We assessed spontaneous cell firing by recording action currents in cell-attached condition to avoid perturbation of the intracellular medium[30]. Average firing frequencies were evaluated within 1 min time bins, before, during, and after peptide application. Recovery was then followed for at least 10 min. Representative traces are shown in **Fig. 1a-c (left panels)**. Comparison of the average results obtained in different conditions is given in **Fig. 1a-c (right panels)**. Insets give the fractional effects of the indicated OX peptides in individual cells, for an appreciation of the cell-to-cell variability. Consistent with previous results in VTA slices[23], OXA (100 nM) increased spontaneous activity in approximately 70% of tested cells (**Fig. 1a**) with a slow recovery. In contrast, 100 nM OXB (**Fig. 1b**) generally decreased DA^{VTA} cell firing frequency within 1-2 min by 20-25%, and recovery was relatively rapid upon peptide removal. A more robust effect was observed using the more specific OX_2R agonist [Ala^{11},D-Leu^{15}]-Orexin B (OXB-AL[31]) at 200 nM, which on average approximately halved DA^{VTA} cell firing rate (**Fig. 1c**).

As OXB is reported to bind poorly OX_1R and only bind OX_2R with high affinity, we next assessed OXB response of DA^{VTA} dissociated from *Hcrtr2*$^{\Delta/\Delta}$ mice, that lack the *Hcrtr2* gene, and thus OX_2R, in all cells[19]. 100 nM OXB was found to only exert minor effects on DA^{VTA} cells (**Fig. 1b, right**), validating the largely OX_2R-dependent effect of OXB.

While these findings confirm that OXA increases DA^{VTA} neuronal firing, they also newly reveal that OXB-mediated OX_2R signaling can induce a transient decrease in DA^{VTA} cell firing. Deletion of *Hcrtr2* in DA^{VTA} neurons would thus be expected to relieve an inhibitory component of OX signaling. The behavioral implication of this finding can be further studied in our previously reported mice engineered to selectively lack the *Hcrtr1* or *Hcrtr2* gene in DA cells[19].

Dopaminergic *Hcrtr1* ablation reduces explorative behavior and reactivity to novelty in an open field.

We previously showed that genetic inactivation of *Hcrtr2*, but not *Hcrtr1*, or compound inactivation of both receptors, in DA neurons, causes mice to exhibit a dramatic increase in time spontaneously spent in

an EEG theta-enriched alert substate of wakefulness (often referred to as 'active wakefulness' in rodents, as it can be, but not always is, associated with locomotor activity)[9,19]. In a reward-driven operant conditioning paradigm based on visual discrimination, the altered waking state of $DA^{Ox2R\text{-}KO}$ mice was found to be associated with an increased learning rate and improved attentional performance. This was however also accompanied by deficits in impulse control, with compulsive and impulsive-like behaviors[19]. To further explore the impact of inactivating OX->DA pathways, we experimented cohorts of $DA^{Ox1R\text{-}KO}$, $DA^{Ox2R\text{-}KO}$, and their respective genetic control littermates ($DA^{Ox1R\text{-}CT}$ and $DA^{Ox2R\text{-}CT}$) in an extended battery of behavioral tests.

To evaluate the role of OX→DA pathways in locomotor and explorative behaviors, mice were first exposed to a 10-min open field test (**Fig. 2a, Left)**. While $DA^{Ox1R\text{-}KO}$ and $DA^{Ox1R\text{-}CT}$ mice covered a similar total distance within the arena (**Fig. 2c, Left**), $DA^{Ox1R\text{-}KO}$ mice spent more time in the wall zone and less time in the center zone respective to controls, suggesting increased thigmotaxis[32] and anxiety-like behavior (**Fig. 2b-c**). Immediately following the 10-min open field test, a small object was placed in the middle of the center zone and mice were allowed a further 5 min of free exploration (**Fig. 2a, Right**). Again, $DA^{Ox1R\text{-}KO}$ mice spent less time in the center zone of the open field, as well as in the center zone restricted to the object proximity (**Fig. 2e**). In contrast, $DA^{Ox2R\text{-}KO}$ and $DA^{Ox2R\text{-}CT}$ mice displayed no differences in total distance traveled, time sent in the wall or center zones (**Fig. S1a-b**), nor in exploration of the novel object (**Fig. S1c-d**). Altogether, our data reveal that $DA^{Ox1R\text{-}KO}$ mice show increased anxiety-like behavior during exploration of an open field arena, and reduced approach towards an object placed in the most anxiogenic zone of the open field.

Dopaminergic *Hcrtr1*-ablated mice show hyperactivity and atypical behavior in the elevated plus maze

Because reduced exploration of the open field suggests heightened anxiety-like behavior, we next evaluated our mice in the elevated plus maze (EPM) test, a test widely used to assay anxiety in rodents (**Fig. 2f**). $DA^{Ox1R\text{-}KO}$ showed increases in total distance traveled (**Fig. 2g**) and total number of zone crossings (**Fig. 2h** compared to $DA^{Ox1R\text{-}CT}$ mice, but no other change in time spent in the open or closed arms of the maze (**Fig. 2i-j**). Hence, loss of dopaminergic *Hcrt1* induces a context-dependent hyperactivity, manifested by enhanced zone crossing behavior in the elevated plus maze.

No differences were observed between $DA^{Ox2R\text{-}KO}$ and $DA^{Ox2R\text{-}CT}$ mice in the elevated plus maze test (**Fig. S1e-h**), consistently with the open field test data, indicating no alterations in locomotion or anxiety-like behavior.

Previous studies suggest that OX modulation of DA neuronal targets is critical in risk assessment[33], as well as in executive control, including impulsive and compulsive-like behavioral patterns[19]. Because the EPM test shows a one trial tolerance effect, meaning that normal mice exposed to a 2nd EPM trial display an almost total avoidance of open arms[34 35,36], we asked whether exposing our mutant mice to a 2nd EPM exposure might reveal behavioral alterations, indicative of alterations in risk assessment, impulse control, or in the phobic-like avoidance of open arms[37,38]. Thus, 24 h after the 1st elevated plus maze trial, we exposed mice to a 2nd trial. As expected from prior reports, the total distance traveled was reduced between the 1st and 2nd trials in both $DA^{Ox1R\text{-}KO}$ and $DA^{Ox1R\text{-}CT}$ mice. However, interestingly, whereas $DA^{Ox1R\text{-}CT}$ mice show, as expected, decreased time spent in the open arms during the 2nd trial compared to the 1st, $DA^{Ox1R\text{-}KO}$ mice did not show any difference between trials 1 and 2 (**Fig. 2k-l**). In contrast, both $DA^{Ox2R\text{-}KO}$

and DA$^{Ox2R\text{-}CT}$ showed the expected pattern of reduced time in open arms during the 2nd trial relative to the 1st (**Fig. S1i-l**). This result suggests a role of OX_1R signaling in DA neurons for behavioral adaptation and acquisition of phobic-like responses.

Altogether, our findings support a specific role of signaling by OX_1R, but not OX_2R, in DA neurons for exploration of an open arena, or a novel object in this arena. Because the EPM 1st trial anxiety-like responding was not different in DA$^{Ox1R\text{-}KO}$ than in control mice, our data suggest that DA$^{Ox1R\text{-}KO}$ mice exhibit context-dependent heightened anxiety-like behavior, that selectively manifests in open field arenas.

Dopaminergic *Hcrtr2*-ablated mice show reduced sociability.

Given the important role of DA[39-41] and OX [42,43] neurons in social behavior, we asked whether loss of *Hcrtr1* or *Hcrtr2* from DA neurons alters the social interaction domain and approach behavior. In the three-chamber sociability test[44], after 10 min of free exploration and habituation to the arena, mice can explore an empty enclosure or an enclosure containing a non-familiar juvenile mouse (**Fig. 3a**). We found that DA$^{Ox1R\text{-}KO}$ mice manifest increased locomotion compared to controls during the habituation phase (when no enclosures were present). This manifested with an increased total distance traveled (**Fig. 3b**), and increased number of inter-chamber-crossings of DA$^{Ox1R\text{-}KO}$ vs DA$^{Ox1R\text{-}CT}$ mice (**Fig. 3c)**. During the test, both DA$^{Ox1R\text{-}KO}$ and DA$^{Ox1R\text{-}CT}$ mice showed intact sociability, with a larger % of time spent in proximity to the juvenile mouse than the empty enclosure (**Fig.3e-f**), and a longer average exploration bout duration around the social than the inanimate stimulus (**Fig.3g-h**).

In contrast to DA$^{Ox1R\text{-}KO}$ mice, DA$^{Ox2R\text{-}KO}$ mice manifested no hyperlocomotion, i.e., no differences in total distance traveled (**Fig. 3i**), nor in number of inter-chamber crossings (**Fig. 3j**) during the habituation phase relative to DA$^{Ox2R\text{-}CT}$ controls. Remarkably, however, while DA$^{Ox2R\text{-}CT}$ mice showed a clear preference for the juvenile mouse vs the empty enclosure, DA$^{Ox2R\text{-}KO}$ mice did not (**Fig. 3k-m**). Additionally, DA$^{Ox2R\text{-}CT}$ mice showed longer mean exploration bout durations for the juvenile mouse rather than for the object (**Fig. 3n**), while DA$^{Ox1R\text{-}KO}$ did not (**Fig. 3o**). These data reveal a critical role of OX_2R-mediated modulation of DA neuronal activity for expression of social preference in mice.

Dopaminergic *Hcrtr1*-ablated mice exhibit increased impulsive and compulsive responding during training in a reward-driven learning task

Mice were first exposed to an operant conditioning learning task equivalent to the Continuous Attention Performance Task in humans, namely the 3-Choice Serial Reaction Time task (3-CSRTT), measuring sweet reward-driven instrumental learning, attentional skills, as well as compulsivity and impulsivity-like parameters[45]. We previously reported that, in a similar task, DA$^{Ox2R\text{-}KO}$ mice exhibit a markedly enhanced learning rate, and improved baseline accuracy, indicating higher attentional skills once performance was stabilized and test contingencies were made more difficult. This improved performance was, however, accompanied by maladaptive patterns of reward-seeking, with presence of compulsive and impulsive-like responses[19].

In a similar version of the 3-CSRTT procedure (**Fig. 4a**), also comprising mild food restriction (see Materials and Methods for details), DA$^{Ox1R\text{-}KO}$ and DA$^{Ox1R\text{-}CT}$ mice manifested no weight differences before food restriction (**Fig.4c**), at experimental start (**Fig. 4d**) or throughout the learning process (**Fig. 4b**. DA$^{Ox1R\text{-}KO}$ and DA$^{Ox1R\text{-}CT}$ mice also showed similar learning rates from one stage to the next (**Fig. 4e**). However,

during the first 10 training days, DA$^{Ox1R\text{-}KO}$ mice completed a higher number of total trials (**Fig. 4f**), a higher number of premature responses (**Fig. 4k**), a higher number of incorrect responses (**Fig. 4g**), although no differences in number of correct responses, response accuracy or response omissions relative to controls (**Fig. 4h-j**). In addition, compared to controls, DA$^{Ox1R\text{-}KO}$ mice showed an increased number of repetitive responses in the nosepoking apertures (**Fig. 4l**), as well as a trend toward higher repetitive nosepoking responses in the food magazine (**Fig. 4m**). Repetitive nosepoking responses in the apertures or the food magazine are considered indices of compulsive behavior[45].

Therefore, both DA$^{Ox2R\text{-}KO}$ and DA$^{Ox1R\text{-}KO}$ mice show compulsive behavioral patterns, suggesting that dopaminergic cell OXR signaling may be protective for such traits. Additionally, although both mutant lines show compulsive-like responding, it is seen in the context of a task marked by pronounced increases in cognitive performance, i.e., improved learning speed and response accuracy, only in DA$^{Ox2R\text{-}KO}$ mice.

After evaluating reward-driven learning, we next assessed aversion-driven learning, and specifically, fear-based associative learning, using the active avoidance task (**Fig. 5a**). We investigated DA$^{Ox1R\text{-}KO}$ mice' ability to learn to avoid an electric shock preceded by a 10-s-long tone by transiting to another chamber, across a 2-day learning procedure. DA$^{Ox1R\text{-}KO}$ and their controls displayed similar performance in learning the active avoidance task, i.e. similar numbers of successful shock avoidances (i.e., transitioning to the other chamber during the shock-predicting tone, **Fig. 5d**), escapes (i.e. transitions to the safe chamber after the shock had commenced, **Fig. 5f**), and premature responses (transitions to the chamber before the tone had started, **Fig. 5b**). DA$^{Ox1R\text{-}KO}$ mice however showed a shorter latency to avoid the shock on day 1 (**Fig. 5e**). Altogether, our findings suggest that loss of OX_1R-mediated modulation of DA cell activity affects impulse control in a reward-driven operant conditioning task, leading to maladapted behaviors that include impulsive and compulsive responding. Avoidance-driven learning appears however normal in DA$^{Ox1R\text{-}KO}$ mice, with the exception that they exhibit faster reaction times in avoidance responding than do controls. Whether this feature reflects an impulsive component, alteration in risk assessment, or some other effect of OX1R loss is presently unknown.

Dopaminergic *Hcrtr2*-ablated mice show impaired aversion-based instrumental learning

As mentioned above, DA$^{Ox2R\text{-}KO}$ mice exhibited faster learning and improved baseline performance in a reward-driven, visual-discrimination-based, operant conditioning task[19]. In contrast, in this study we found that DA$^{Ox2R\text{-}KO}$ mice exhibited severely compromised aversive stimulus-based learning in the Active Avoidance test (**Fig. 5a**). Thus DA$^{Ox2R\text{-}KO}$ mice showed a lower number of successful avoidances, i.e., transitions in the adjacent chamber during the conditioned stimulus (tone) and before electric shock start Fig. **5l**), and underwent more electric shocks, as they showed a higher number of escapes, i.e., higher inter-chamber runs after completion of the 10-s tone conditioned stimulus and the electric shock had started Fig. **5n**). DA$^{Ox2R\text{-}KO}$ and DA$^{Ox2R\text{-}CT}$ mice showed no differences in premature responding (**Fi. 5j**).

As DA$^{Ox2R\text{-}KO}$ mice showed shorter escape latency in day 1 of learning (**Fig. 5o**), and increased number of escapes, these data suggest that DA$^{Ox2R\text{-}KO}$ mice still perceive the electric shock as an aversive stimulus, and DA$^{Ox2R\text{-}KO}$ mice's poor aversive learning skills are not secondary to a sensory deficit (Razavi 2017).

Furthermore, our prior study demonstrated impulse control deficits in mice with loss of OX_2R signaling in DA neurons[19]. Hence, interestingly, the mice' hyperaroused EEG appears to put them at an advantage in attention for positively-valenced stimuli[19], but not for negatively-valenced stimuli. The association in

$DA^{Ox2R\text{-}KO}$ mice of opposite performance scores in reward- vs avoidance-driven learning tasks suggests differential downstream effector involvement.

Our results altogether demonstrate that dopamine neuron-selective genetic disruption of *Hcrtr1* or *Hcrtr2* profoundly differentially affects socioemotional behaviors in mice. This suggests the existence of previously unrecognized major differences between OX_1R and OX_2R signaling in DA neurons. We therefore next investigated the cellular bases of these differences by measuring how OXA, and OXB impact the excitability of DA^{VTA} cells, and whether action of orexins is altered in $DA^{Ox1R\text{-}KO}$ and $DA^{Ox2R\text{-}KO}$ mice.

Opposite effects of OX_1R and OX_2R activation on DA^{VTA} firing *ex vivo*: OXA increases DA^{VTA} cell firing in slices from control, but not $DA^{Ox1R\text{-}KO}$ mice, while OXB decreases DA^{VTA} cell firing in slices from control, but not $DA^{Ox2R\text{-}KO}$ mice.

First, we assessed intrinsic excitability of DA^{VTA} cells from $DA^{Ox1R\text{-}KO}$ and $DA^{Ox1R\text{-}CT}$ mice through patch-clamp recordings in DA neurons of the lateral VTA (**Fig. 6a**, see criteria for cell identification in Materials and Methods), as this region contains NAc-projecting DA cells shown to be modulated by orexins[46]. When cell firing was elicited by depolarizing current injections (**Fig. 6a-b**), no differences were observed in the firing frequency-injected current relationships between $DA^{Ox1R\text{-}KO}$ and $DA^{Ox1R\text{-}CT}$ mice (**Fig. 6c**), indicating that OX_1R loss did not alter basal intrinsic excitability of DA^{VTA} cells. To study the impact of orexin release on intrinsic excitability, we bath-applied orexin peptides and measured the changes in firing of DA^{VTA} cells elicited by brief depolarizations of constant amplitude[46]. As OXA binds OX_1R with high affinity[2,11], slices from $DA^{Ox1R\text{-}KO}$ and $DA^{Ox1R\text{-}CT}$ mice were perfused with OXA (100 nM) for 5 min after a 10 min baseline (**Fig. 6d-e**). Whereas OXA increased the firing rate in control mice, it had no effect in $DA^{Ox1R\text{-}KO}$ mice (**Fig. 6e-f**). Higher firing upon OXA perfusion in control cells was abolished by OX_1R-blockade using the selective antagonist SB-334867, indicating that OXA-induced DA^{VTA} cell firing increase is OX_1R-dependent (**Fig. S3**). Our observations are consistent with reports of Baimel *et al*[46], who showed that OXA increases the firing of lateral NAc-shell-projecting DA neurons in an OX_1R-dependent manner (i.e., prevented by OX_1R blockade), and that this effect is cell-autonomous (i.e., preserved if Glutamatergic and GABAergic synaptic receptors are blocked). Since DA neurons from $DA^{Ox1R\text{-}KO}$ mice should still at a high rate express the OX_2R-expressing *Hcrtr2* gene[19], the absence of effect of OXA exposure also suggests that OXA-driven OX_2R signaling is not significantly contributing in modulating the firing rate of DA cells.

To next assess the intrinsic excitability properties of DA^{VTA} cells lacking *Hcrtr2*, we followed a similar methodology as above and assessed the response of cells from $DA^{Ox2R\text{-}KO}$ and $DA^{Ox2R\text{-}CT}$ mice to bath-applied OXB, as OXB binds OX_2R with high affinity but only poorly OX_1R[2,11]. No differences in basal intrinsic excitability were observed between cells from $DA^{Ox2R\text{-}KO}$ and $DA^{Ox2R\text{-}CT}$ mice (**Fig. 7b-c**). Strikingly, and consistently with the results from dissociated VTA cells, we found that OXB decreased firing of DA^{VTA} neurons from control mice (**Fig. 7e-f**). This decrease was abolished in DA^{VTA} cells of $DA^{Ox2R\text{-}KO}$ mice, lacking an active *Hcrtr2* gene, thus validating the $DA^{Ox2R\text{-}KO}$ mouse model, while indicating that the OXB-induced decrease in cell firing observed in control mice is OX_2R-dependent. In fact, DA^{VTA} cells of $DA^{Ox2R\text{-}KO}$ mice showed a tendency towards increased firing upon OXB exposure (comparison between number of spikes pre- *vs* post-OXB spike in KO: P=0.077, **Fig. 7e**). This may reflect preserved OX_1R signaling in $DA^{Ox2R\text{-}KO}$ mice activated by OXB, despite the reported lower binding affinity of OXB for OX_1R. Importantly, these data align

with those described above in acutely dissociated DA^{VTA} cells, and indicate that OXB has an inhibitory action on lateral DA^{VTA} cell excitability, which is opposite to the action of OXA.

To corroborate this finding and confirm that the OXB effect is cell-autonomous in VTA slices and dependent on OX_2Rs, we performed experiments in C57BL/6J WT mice. Consistent with our results in $DA^{Ox2R\text{-}CT}$ mice, OXB decreased the firing rate of DA^{VTA} cells from WT mice. This effect was prevented by OX_2R blockade with TCS-OX2-29 (**Fig. 7h-i**) but persisted in the presence of antagonists for ionotropic synaptic receptors (**Fig. 7h-i**), ruling out possible indirect actions of OXB on DA^{VTA} cells' excitability, e.g., via for instance glutamatergic transmission[26].

These data indicate that OXA and OXB peptides exert opposite actions on DA^{VTA} cells' intrinsic excitability, and their impact is lost in our $DA^{Ox1R\text{-}KO}$ and $DA^{Ox2R\text{-}KO}$ mouse models, respectively.

DISCUSSION

Both OX and DA serve as major neural hubs for the processing of past and present salient information, contributing to the proper regulation of arousal, motivational states, and stress responses. Growing evidence supports their involvement in both appetitive and aversive behavioral paradigms[47-50]. Their interactions are less well studied due to the inherent difficulties in simultaneously interrogating their functions *in vivo*. Even less is known about the specific contributions of OX_1R and OX_2R.

To probe the functional roles of the two receptors in OX→DA connectivity, we generated mice whose DA neurons are unable to respond to orexins by selective genetic deletion of *Hcrtr1* or *Hcrtr2* in DA cells[19]. Systematic analysis of the mice' EEG activity, sleep/wake vigilance state variables and architecture revealed that DA-specific *Hcrtr2* loss causes a dramatic increase in time spent in a high-alertness type of wakefulness with enhanced EEG theta-gamma coupling. This was paired with a markedly improved performance in a continuous attention operant task, albeit also with compulsive and impulsive behaviors[19]. We here extend our study of the contribution of orexin signaling in DA neurons to other behavioral domains. Moreover, based on the evidence pointing to modulation of DA^{VTA} neurons as a central component of OX/DA interactions, we interrogate the underlying DA^{VTA} cell electrophysiological substrates.

Inactivating OX_1R or OX_2R in DA neurons induced strikingly different behavioral effects, that we analyze and interpret in the following paragraphs.

$DA^{Ox1R\text{-}KO}$ mice behavior.

These mice displayed a context-specific motor hyperactivity, accompanied by marked impulsivity and repetitive behaviors. This was manifested by increased total distance traveled and inter-zone crossings in both the elevated-plus-maze, and the 3-chamber apparatus, as well as an increase in total trials completed, the numbers of premature, incorrect, and perseverative responses during the training phase of the 3-CSRTT. Also observed were potential indices of impaired risk assessment. These included an atypical responding pattern in the EPM 2nd trial, performed 24 h after the 1st EPM trial, with lack of the commonly observed decreased exploration of open arms in trial 2 *vs* 1, which may suggest alterations in behavioral adaptation patterns and deficits in acquisition of phobic-like responses[37,38], and faster reaction times in active avoidance responding. Furthermore, context-dependent reduction of exploratory behavior

and novel object approach in the center of an open field were observed, suggesting augmented anxiety-like behavior.

Specifically, compared to controls, DA$^{Ox1R\text{-}KO}$ mice engage in increased exploration and locomotion in confined arenas (such as the EPM or the chambers of the sociability arena), but this hyperlocomotion was not evident in larger open areas, namely the open field (45 x 45 cm). Exploration of an open field implicates locomotor, motivational and emotional aspects[49], while the EPM is one of the most commonly used tests to study anxiety-like behavior in rodents[51]. Our data suggest anxiety-like responding in the open field, but not the EPM. Dissociation between results observed in the open field and EPM was previously reported by others[52]. Such context-dependent difference in anxiety-related characterization may stem from several causes. First, the open field was the first paradigm we subjected our mice to in our behavioral test pipeline (see Materials and Methods). Thus, despite the handling procedure adopted to habituate the mice to the experimenter before behavioral tests, anxiety-like behavior could have decreased as mice gradually accustomed to experimental testing. Moreover, the two tests may measure different aspects of anxiety-like behavior[53]. Furthermore, parameters such as task duration (10 min in OF, 5 min in EPM), differences in spatial configuration, or in temporal habituation to the specific environments may also be involved in the divergent readouts of the tests. The EPM one-trial tolerance effect[34], observed in all but the DA$^{Ox1R\text{-}KO}$ mouse group, suggests involvement of pathways selectively downstream of DA OX_1R signaling in this effect. The EPM one-trial tolerance effect was previously reported to involve NMDAR activation and inactivation of D1-like Rs in several areas including the hippocampus[36].

Our observation of reduced exploration in the open field in DA$^{Ox1R\text{-}KO}$ mice misalign with reports by Xiao *et al*[54] describing increased novelty-induced locomotion and exploration in the open field in a similar but distinct model of selective *Hcrtr1* disruption in DA neurons. These discrepancies may stem from several factors. First, the mouse model used by Xiao *et al* substantially differs from ours in several ways. While *Hcrtr1* gene is predominantly expressed in DA^{VTA} cells of their mice, we showed that >80% of TH^{+} cells in the ventral midbrain of our mice (in a C57BL/6N X C57BL/6J genetic background) express both *Hcrtr1* and *Hcrtr2* genes[19]. Most critically, Xiao et al used a different *Dopamine transporter* (*Dat*)-Cre driver allele[55], which, unlike ours[56], lacks an IRES, thus is a *Dat* gene KO. Xiao et al's DA-*Ox1R*-KO mice are therefore heterozygous for the *Dat* gene, while our DA$^{Ox1R\text{-}KO}$ mice are not. Reduced *Dat* expression is well documented to lead to increase DA levels and locomotor hyperactivity[57] and heterozygous Dat-Cre mice lacking an IRES show locomotor hyperactivity[58], which could explain some of Xiao *et al*'s observations. Backman *et al*[56] in contrast showed that extracellular DA levels are not significantly altered in the brain of *Dat*$^{+/ires\text{-}Cre}$ mice, and we showed that *Dat*$^{+/ires\text{-}Cre}$ mice in absence of any *Hcrtr* allele show normal locomotor activity as *Dat*$^{+/+}$ mice[59]. Second, Xiao *et al* used an OF arena measuring 27 × 27 cm, while ours was 45 x 45 cm, thus considerably larger, potentially explaining reduced OF exploration in our case. Lastly, while we found reduced exploration of DA$^{Ox1R\text{-}KO}$ mice in large open fields, we also showed that the mice display hyperactivity in selected more confined arenas.

Further experiments are warranted to investigate whether the lack of behavioral adaptation of DA$^{OX1R\text{-}KO}$ mice in the 2nd EPM trial could reflect altered risk assessment. The interpretation of impaired risk-assessment in DA$^{OX1R\text{-}KO}$ mice may align with the fact that the activity of NAc D_2 cells participate in avoidance of learned risks[60], and excitation of NAc^{D2} cells by OX is critical for mice to express innate risk avoidance, in their case upon exposure to fox urine-derived odorants[33]. Of note, OX can act by postsynaptic

but also extra-synaptic action, i.e. acting on cell somata, neurites or axon terminals. In terminals, OX can modulate release of neurotransmitters, e.g. glutamate, GABA, and DA[61-64]. Thus the effects of our mutations can also be exerted by loss of OXRs expressed on DA cell terminals, such as here on accumbal DA terminals[61,62].

In terms of learning, $DA^{OX1R\text{-}KO}$ mice successfully learned the active avoidance test, showing equal number of avoidance responses (which is used as a learning proxy in this task) and a faster reaction time to avoid the shock upon presentation of the conditioned stimulus compared to control mice. Regarding training in the 3-CSRTT, a continuous performance task, $DA^{OX1R\text{-}KO}$ mice showed increased impulsive and compulsive responding compared to their control littermates.

Altogether, the traits displayed by $DA^{Ox1R\text{-}KO}$ mice, hyperactivity in the EPM 1st trial or 3-chamber arena, atypical exploration in EPM 2nd trial, premature and repetitive responding in the 3-CSRTT, shorter avoidance latencies in the active avoidance test, as well as reduced exploration and novelty-seeking in open fields, could reflect a general deficiency or alteration in information processing. In particular, DA^{VTA}→PFC mesocortical pathways are thought to calibrate DA levels to optimize signal-to-noise ratios, enhancing the discrimination of relevant sensory stimuli, as well as ensuring appropriate disengagement of motor outputs following decision-making[65-68]. Therefore, $DA^{Ox1R\text{-}KO}$ mice' behavioral deficits may in part reflect inefficient OX stimulation of OX_1R-mediated DA release in these mesocortical pathways. A resulting decreased ability of the mice in discriminating the most salient stimuli may lead to suboptimal goal-oriented and exploratory behaviors and the activation of unfocused motor-related responses, in association with augmented anxiety-like responses.

$DA^{Ox2R\text{-}KO}$ mice behavior.

Our prior and present data show that $DA^{Ox2R\text{-}KO}$ mice exhibit a complex phenotype, with a combination of pronounced strengths but also weaknesses relative to their control littermates. On one hand, these mice exhibit a dramatic increase in EEG markers of alertness, enhanced EEG theta-gamma phase-amplitude coupling, in association with markedly improved learning speed and attentional accuracy skills at baseline in a reward-driven operant conditioning learning task 3-CSRTT[19]. On the other hand, these cognitive advantages are accompanied by impaired impulse control[19]. Here we furthermore showed that superior reward-learning is accompanied by compromised aversion-driven instrumental learning. Hence, the hyperaroused EEG activity and the enhanced theta-gamma coupling of $DA^{Ox2R\text{-}KO}$ mice appear to be linked to an advantage in some tasks (attention for stimuli with positive valence) but not others (learning negatively-valence cues), highlighting the potential distinct effector pathways involved in reward vs aversive learning.

Enhanced learning and attentional performance in baseline 3-CSRTT conditions could be a response of enhanced DA^{VTA} activity, resulting from the constitutive loss of an OX_2R-dependent brake on DA^{VTA} activity, as discussed below. It has been documented that alterations in activation of DA neurons can disrupt aversive conditioning and increase trauma-related generalized anxiety-like responses[69].

Contingency awareness, or learning to link external cues' contingencies to aversive outcomes, appears DA-dependent and is a critical factor determining generalized anxiety-like traits. For instance, voltammetry recordings in the ventral striatum showed that differences in DA levels are associated with behavioral outcomes in active avoidance tests, with DA modeled to encode a safety prediction error signal[70].

DA^{VTA}→mPFC projections moreover participate in active avoidance learning[71]. Although we do not yet here demonstrate the downstream effectors of the effects we observe, our data clearly suggest that signaling via OX_2R, rather than OX_1R, in DA cells is critical for active avoidance learning.

Finally, according to our data in male mice, loss of OX_2R, but not OX_1R, signaling in DA neurons results in reduced social interaction as assessed in the 3-chamber social preference task. In general, DA dynamics and the mesolimbic system participate in social behaviors[41,72,73], and optogenetic inhibition of OX neurons reduces social interaction in male mice[42]. However, use of knock-out mice[43] and specific pharmacological antagonists[42] implicated OX_1R in such effects. Future experiments will assess the contribution of OX_1R and OX_2R signaling in DA neurons in social paradigms different from the one adopted here.

$DA^{Ox2R\text{-}KO}$ mice overall display several endophenotypes reminiscent of mouse models of autism spectrum disorder (ASD). Although the use of the mouse as an ASD model is challenging, even controversial[74,75], aspects of $DA^{Ox2R\text{-}KO}$ mice, namely enhanced performance in specific forms of learning but not others, repetitive responding and altered social interactions may be seen to align with behavioral features modeled in ASD mouse models. Because alterations in DA^{VTA}-NAc/mPFC pathways are increasingly reported to cause manifestations related to autism spectrum disorders[76,77], probing $DA^{Ox2R\text{-}KO}$ mice' DA^{VTA}-NAc/mPFC circuits for sites of altered DA release may help define the circuit-mechanisms underlying their behavioral abnormalities.

Pronounced compulsivity was the only behavioral characteristic revealed to be common between $DA^{Ox1R\text{-}KO}$ and $DA^{Ox2R\text{-}KO}$ mice. Impaired executive control in the form of premature and repetitive responding thus represents a point of convergence in the distinct effects of disrupting OX→DA pathways.

Linking *in vivo* mouse characteristics with *ex vivo* DA^{VTA} cell electrophysiology

The contrasting behavioral phenotypes of $DA^{Ox1R\text{-}KO}$ and $DA^{Ox2R\text{-}KO}$ mice suggest that OX_1R and OX_2R receptors contribute differently to dopaminergic cell activity and eventually dopaminergic synaptic circuits. To assess whether OX_1R and OX_2R produce distinct electrophysiological effects on DA^{VTA} cells, and to isolate cell-autonomous responses independent of cellular network effects implicating non-dopaminergic VTA cell types, we first performed patch-clamp recordings of DA cells acutely dissociated from brain VTA slices. In addition, we conducted patch-clamp recordings of DA cells in VTA slices of WT and our mutant lines. To address mesolimbic pathways, we recorded DA neurons of the lateral VTA, which preferentially project to the NAc shell and respond to OXA with increased firing[46]. In both experimental conditions, we aimed at isolating alterations in intrinsic excitability of DA^{VTA} neurons in response to OXs. Thus, in VTA slices, we did not assess spontaneous firing but stimulated the cells to fire at regular successive timepoints. Forcing the cells to fire highlights the contribution of altered intrinsic excitability.

In both preparations, we found differential effects of OXA vs OXB, with OXA increasing cell firing in WT or controls, but not $DA^{Ox1R\text{-}KO}$ mice. This indicates that, although OXA is reported to bind equally well OX_1R and OX_2R, the DA^{VTA} cell response to OXA is primarily OX_1R-driven, consistently with previous results showing that the OXA effect on DA^{VTA} cell firing is blocked by the OX_1R antagonist SB-33487[46]. On the other hand, OXB or the OX_2R-selective agonist OXB-AL, induced a transient inhibitory and OX_2R-dependent response. In DA^{VTA} cells of $DA^{Ox2R\text{-}KO}$ mice, the firing decrease produced by OXB in control mice was prevented, and a tendency towards increased firing was observed, potentially explained by a residual degree of response of OX_1Rs to OXB. Although OX_2R signaling mediates an excitatory action in most cells

including histamine neurons[78], heterogeneity in OXR mechanisms of signal transduction in different neuronal types is well known[79], and inhibitory effects of OXR signaling are not unprecedented (see below).

These results support the notion that OXA-induced OX_1R signaling in DA^{VTA} cells stimulates cell firing, whereas OXB-mediated OX_2R signaling produces a decrease. Consequently, deletion of *Hcrtr2* in DA^{VTA} neurons should relieve an inhibitory component of OXR signaling and thus facilitate OX excitatory effects. This is consistent with the observation that $DA^{Ox2R\text{-}KO}$ mice exhibit EEG theta-enriched states of wakefulness and REMS, and our prior hypothesis that this theta power increase stems from relief of inhibition of the VTA-septo-hippocampal pathways that generate theta activity[19]. Moreover, our findings that OXA enhances DA^{VTA} neuron firing predominantly via OX_1R, whereas OXB decreases firing through OX_2R suggests that OX_1R activation promotes reward-related behaviors, while OX_2R activity may counterbalance excessive excitation to maintain behavioral flexibility.

Although OX peptides are primarily thought to exert a neuroexcitatory activity, inhibitory effects of OXR signaling have been evidenced in POMC, SCN, and a subset of MCH neurons[80-83]. The intracellular mechanisms by which OX_2R signaling cause an intrinsic inhibitory effect in DA^{VTA} neurons remain to be determined. K^+ channels[82], in particular small conductance calcium-activated K^+ (SK/K_{Ca}) channels[84], are plausible candidate targets. In this line, we note that recent results suggest that modulating K_{Ca} currents that inhibit DA^{VTA} cell firing can regulate some autistic-like manifestations in murine models[85].

Our results may appear in partial conflict with those of Korotkova *et al*[23], reporting increased DA^{VTA} cell firing by both OXA and OXB in VTA slices from 3-4-week-old Wistar rats. These authors, however, recorded spontaneous firing. In such conditions, DA cell firing results from integration of cell-autonomous effects combined with exogenous contributions, such as local GABAergic input as well as terminals from mPFC glutamatergic afferents. Additionally, while our slice recordings targeted putative NAc-projecting neurons, Korotkova *et al*[23] did not attempt output specificity.

As DA^{VTA} cells (A10 DA neurons) are the best characterized dopaminergic OX target, we directed our electrophysiological recordings to the VTA. However, other potential target DA groups in hypothalamus (hypothalamic A11-A15 DA neurons) or dorsal raphe nucleus (DRN) are implicated in vigilance regulation and behavioral phenotypes[86,87,88]. Korchynska *et al*[88] described a hypothalamic DA locus implicated in psychostimulant-induced hyperlocomotion in mice. OX_2R activation in DRN DA neurons may contribute to stress resilience and arousal regulation. The responses of nigral DA cells to OX peptides remain controversial[29,89,90]. Systematic analysis of different DA cell groups to assess their respective involvement in the behavioral phenotypes we observed is warranted.

Our findings nonetheless highlight striking differential effects of the two OX peptides and the two OX receptors on DA^{VTA} cells. Further investigations into the molecular mechanisms and downstream intracellular targets of these effects will explore the potential differential dynamics of OX_1R and OX_2R signaling, and, importantly, assess how OXA and OXB compete *in vivo* to exert their opposing modulation of DA^{VTA} cell activity.

Conclusions: implications for neuropsychiatry

Our data establish a genetically-defined link between monosynaptic OX→DA neurotransmission and disease-relevant socio-emotional behaviors and executive cognition. Most importantly, we evidence an

unprecedented dichotomy in the functions of OX_1R and OX_2R in processes altered in several neuropsychiatric disorders, such as obsessive-compulsive, attention-deficit/hyperactivity, and autism-spectrum disorders. Because the DA system is centrally affected in most neuropsychiatric disorders and several major common neurological diseases, distinguishing the direct OX modulation of the DA system from that exerted by other systems has great translational potential.

For instance, as we show that OXB and OX_2R agonists can induce, at least transiently, diminished DA^{VTA} neuronal excitability, they could contribute to aggravate cataplexy, since D2 agonists known to inhibit DA^{VTA} neurons do aggravate cataplexy[91]. OX_2R agonists are however reported to suppress cataplexy[92], suggesting that the DA system is not a primary target of OX_2R agonists, or at least not in most contexts that were assessed. Considering the role of the mPFC in cataplexy[93,94], a potential explanation is that OX_2R agonists exert their effect on cataplexy mainly through neocortical receptors. As to OXR antagonists, dual OXR antagonists (DORAs) are already used for the treatment of insomnia, and OX_1R antagonists (SO1RA) are gaining interest for their potential use in the treatment of several CNS disorders, including substance abuse, eating, obsessive, compulsive, and anxiety disorders[95,96]. While blocking OX_2R may reduce wakefulness, the expected advantage of selectively antagonizing OX_1R may be the ability to achieve clinical efficacy without sleep promotion.

A thorough understanding of the distinct physiological effects of the two receptors is essential for identifying potential side effects of the expanding class of OXR-interacting drugs. For example, since both $DA^{Ox1R\text{-}KO}$ and $DA^{Ox2R\text{-}KO}$ exhibit a pronounced compulsivity-related endophenotype, DORA-related side effects in this domain should be carefully monitored. Additionally, OX_1R antagonists intended for substance abuse treatment should be evaluated for potential anxiogenic effects. Our findings may therefore have broad implications for the emerging field of OXR neuropharmacology.

Materials and Methods

Animals

Mice were generated and bred as previously described[19]. Briefly, we engineered the *Hcrtr1* (*Ox1R*) and *Hcrtr2* (*Ox2R*) genes to create Cre-dependent knockout/GFP-reporter floxed alleles: $Hcrtr1^{flox}$ and $Hcrtr2^{flox}$ crossed to a Dopamine transporter Cre driver (Dat-IRES-Cre), generating:

$Hcrtr1^{flox/flox};Dat^{+/Cre}$ (abbreviated: $DA^{Ox1R\text{-}KO}$) and $Hcrtr1^{flox/flox};Dat^{+/+}$ ($DA^{Ox1R\text{-}CT}$) controls, and $Hcrtr2^{flox/flox};Dat^{+/Cre}$ ($DA^{Ox2R\text{-}KO}$) and $Hcrtr2^{flox/flox}$ ($DA^{Ox2R\text{-}CT}$) controls.

We therefore generated 4 genotypic groups (2 KO:CT pairs, for *Hcrtr1* and *Hcrtr2*, respectively), and performed all analyses as pair-wise comparisons between KO and CT littermate groups.

For behavioral testing, adult 3- to 6-month-old males were housed in groups of 2-4 animals/cage and maintained on a 12h:12h light–dark cycle (light-on at 07:00 AM). Mice had *ad libitum* access to food and water, except from the cohorts assessed in the 3-Choice Serial Reaction Time Task that were maintained under food restriction according to the procedure described below. The number of mice in each group of the behavioral cohorts is described in detail below (see Behavioral tests). KO and CT littermate mice for the electrophysiology recordings were distinct cohorts, not subjected to any behavioral test. All

experiments performed in Switzerland were conducted in conformity with Swiss national institutional guidelines on animal experimentation and approved by a license from the Swiss Cantonal Veterinary Office Committee for Animal Experimentation (Canton de Vaud). Experiments for *ex vivo* recordings of dissociated VTA cells followed the Italian law (2014/26, implementing the 2010/63/UE) and were approved by the local Ethical Committee and the Italian Ministry of Health (68/2021-PR).

Behavioral tests

Behavioral pipeline: Mice (11 $DA^{Ox1R\text{-}CT}$ and 11 $DA^{Ox1R\text{-}KO}$; 19 $DA^{Ox2R\text{-}CT}$ and 12 $DA^{Ox2R\text{-}KO}$) performed sequentially the open field test, elevated plus maze test, 3-chamber sociability test and active avoidance, with ≥24 h between each test. A separate cohort of 7 $DA^{Ox1R\text{-}CT}$ and 8 $DA^{Ox1R\text{-}CT}$ performed the 3-CSRTT. Rationale for any animal exclusion from behavioral analyses are given in detail under each corresponding behavioral test.

Open field and reactivity to novelty tests: To assess locomotion and exploratory behavior, an open field test adapted from previous studies[91,92] was performed, using a Plexiglas (Length x Width x Height) 45 x 45 x 39.5 cm arena equipped with a ceiling-mounted camera. The test consisted of 2 parts: (1) the mouse is allowed to freely explore the open field for 10 min; (2) as the mouse stays in the open field arena, a small object is then softly brought from the side and placed in the arena center, and the mouse allowed to freely explore the arena and the object for a further 5 min, during which reactivity to the novel object is assessed. The arena was divided in center and wall zones, while for the Novel Object Reactivity test, the center zone was further divided to contain a smaller zone around the object (15 x 15 cm). The behavior was monitored using the video camera and analyzed with a computerized tracking system (Ethovision XT 15, Noldus IT). Entries and time spent in the exploration area (center) and the periphery (wall), as well as the total distance travelled in the arena, were recorded automatically. The light intensity in the arena was adjusted to 12-15 lux. The apparatus was cleaned with 5% Ethanol solution and dried thoroughly after each animal. One mouse out of 11 from the $DA^{Ox1R\text{-}KO}$ group was excluded from this test as it climbed on the object for a prolonged time.

Elevated plus maze: To assess anxiety-like behavior, mice were subjected to the elevated plus maze (EPM) test according to previously published protocols[97,9893,94]. The elevated plus maze consists of a cross-shaped arena with two open arms and two closed arms with walls made of Plexiglas and an open center (80 x 78 x 15 cm), which is elevated 47 cm above ground. In each trial, the mouse is placed in the center facing a closed arm and allowed to freely explore the maze for 5 min. Behavior is monitored using a video camera and analyzed using a computerized tracking system (Ethovision XT 15, Noldus IT). Time spent in the center, open and closed arms, and number of visits (entries) into different arms were recorded automatically. The light intensity was 15-16 lux in the open arms, 5-6 lux in the closed arms and 10-12 lux in the center. The apparatus was cleaned with 5% ethanol solution and dried thoroughly after each animal. One mouse out of 11 from the $DA^{Ox1R\text{-}CT}$ group was identified as an outlier and excluded from this test.

Three-chamber sociability test: We used a social interaction assay comprising a rectangular Plexiglas arena (60 × 30 × 22 cm; Ugo Basile, Varese, Italy) divided into three chambers (each 20 × 30 × 22 (height) cm). The center chamber has doors that the mouse can lift to freely access either other chamber. The

social preference test was performed as previously[44,73 72]. Briefly, each mouse is placed in the arena for a 10 min habituation period, when it is allowed to freely explore the empty arena. After the habituation, 2 fenced enclosures with metal vertical bars (16 cm × 9 cm) are placed in the center of the 2 outer chambers. One enclosure is empty (serving as an inanimate object) whereas the other contains a social stimulus (an unfamiliar juvenile mouse 25 ± 1 day old). The enclosure allows visual, auditory, olfactory, and tactile contact between the experimental mouse and the juvenile. Juvenile mice had been habituated daily to the apparatus and the enclosures for a brief period of time in the 3 days preceding the experiment. During the test, the experimental mouse is allowed to freely explore apparatus and enclosures for 10 min. The position of the empty or juvenile-containing enclosures alternated and was counterbalanced for each trial to avoid any bias effect. Sessions were video-tracked using Ethovision XT (Noldus, Wageningen, Netherlands), providing automated recording of time spent around either enclosure using virtual zones designed around them, total distance travelled, and mouse velocity. The social preference score is defined as the time ratio: social/(social+empty). The arena was cleaned with 5% ethanol and dried between trials. One out of 11 $DA^{Ox1R\text{-}CT}$ was identified as an outlier (ROUT method) and excluded from the social preference analysis. All 12 mice were included in the $DA^{Ox2R\text{-}KO}$ group for sociability, but for 1 out of 12 mice we were unable to calculate the bout duration (duration/bout frequency) as bout frequency was 0 for this animal.

3-Choice serial reaction time task (3-CSRTT): The 3-CSRTT test assesses continuous attention performance in rodents. We used an operant chamber (14.5 x 22 x 18 cm) made of two opposing smooth dark-grey aluminum walls and two opposing transparent Plexiglas walls equipped with iSpy camera and POLY software (Imetronic, Pessac, France). We used a protocol, including shaping, training, baseline and impulsivity assessment, adapted from prior studies[45,99-102]. The mouse has to learn to nosepoke in one of three LED-lit apertures in the time during which the light is on (correct response). Each aperture's light is lit in a pseudo-random manner (the sequence of nosepoke activation appears to be statistically random but relying on a deterministic algorithm; a truly random process could result, for example, in one aperture being active 2,3 or more times in a row, thus potentially creating response biases). Each correct response is followed by delivery of a sucrose pellet (Dustless Precision Pellets® 20 mg, Rodent Purified Diet Chocolate Flavor, Bio-Serv) in the food magazine located on the opposite wall of the chamber. If the mouse does not respond within the timeframe when the light is lit in one aperture, a 'limited hold' (LHD) time period follows, during which the LED light is turned off, but the mouse can still perform a correct or incorrect response. An incorrect response, or an omission to respond when the light is on or during the LHD period, leads to a 5-s time-out (TO) period, when all lights are turned off and no action can be taken. Mice were 14 weeks old at the start of the experiment. During 2 weeks, they were habituated to the experimenters with handling and body weight assessment. Mice were then food-restricted to gradually reach 85% of their initial weight, while respecting the expected weight gain for their age. Specifically, we established a mean weekly weight gain of 0.74 g. Weight was monitored every day or every other day. Once the experiment started and mice started to learn to obtain food pellets, we adjusted their regular chow by subtracting the weight of the pellets consumed during the training sessions.

Shaping stages: In parallel to food restriction, a 'Shaping 1' phase of chamber habituation started when the mice became familiar with the chamber and task contingencies. During this phase, mice received a

food pellet reward when they nosepoked in any of the 3 simultaneously lit apertures. To encourage nosepoking, the stimulus lasted 60 s and there were no incorrect responses or TO periods. To go to the 2nd shaping phase (Shaping 2), the mice had to receive ≥20 pellets. During Shaping 2, the mice had to visit the food magazine to initiate a new trial. The stimulus duration was now 30 s and there were still no TO periods after incorrect responses. Unlike in Shaping 1, in Shaping 2, a correct response led to a 2-s ITI before one of the holes was lit again. In case of omissions, the mouse had to start the trial by visiting the food magazine. The mouse had to receive ≥20 pellets to go to the first training stage (i.e. Stage 1).

Training stages: Each training session lasted 30 min or 100 trials, whichever condition was met first. The procedure followed the steps and sequence described previously[45]. To start a trial, the mouse has to visit the food magazine and then, an ITI of 2 or 5 s (depending on the stage) is presented before one of the apertures is lit. Premature responses (nosepokes during the ITI), incorrect responses, or omissions led to a 5-s TO and has to be followed by a poke in the food magazine to start the next ITI and trial. Correct responses led to the distribution of a pellet, which led directly to the ITI. Training followed 10 different stages of gradually increasing difficulties according to Table S1. Once performance was as stable as possible in the last training stage, a so-called 'baseline' performance for each mouse was determined. One animal from the $DA^{Ox1R\text{-}KO}$ group was removed from the 3-CSRTT analyses as it performed 0 correct responses and showed no learning even after 30 days of training in the task.

Active Avoidance: To evaluate associative aversive learning, we performed an active avoidance paradigm in a two-way shuttle box (Ugo Basile, Italy). Mice learn that a tone (conditioned stimulus; CS, or 'warning signal') precedes a mild electric shock that they can stop by escaping to the adjacent 'safe' chamber[103-105]. Mice were run through 50 trials per day for 2 days. Each trial started with a variable interval (15-45 s) after which a 10-s tone preceded a 0.3 mA electric shock delivered through the floor. The shock stopped immediately when the mouse transitioned to the other chamber or after 5 s. The following readouts were quantified: number of premature responses, defined as transitions to the adjacent chamber during the inter-trial interval (ITI) before the tone had started, number of 'avoidances', defined as transitions to the safe chamber during the tone (i.e., before the shock), and the number of 'escapes', defined as transitions to the safe chamber after the shock had started. Avoidance responses are used as index of learning as they require the mouse to make an association between the CS (tone) and the electric shock. An automatic system registered avoidances, escapes and premature responses. Latencies were measured automatically by the system as the reaction times to avoidance, premature and escape responses. Non-learners were defined as performing fewer than 10 avoidance responses in total over the two training days. Between each trial, the apparatus was cleaned with 5% ethanol and dried.

Patch-clamp electrophysiological recording of dissociated DA^{VTA} neurons

Cells were dissociated from 400 µm-thick acute brain slices prepared from P13 to P18 young mice, following standard procedures[106]. Midbrain coronal slices were cut between +3.88 and +2.92 mm from bregma[107] and left to recover for ≥1 h at 30°C under perfusion with oxygenated solution, containing (mM) 87 NaCl, 21 $NaHCO_3$, 1.25 NaH_2PO_4, 7 $MgCl_2$, 0.5 $CaCl_2$, 2.5 KCl, 25 glucose, 0.4 ascorbic acid, 75 sucrose. The dissociation procedure followed Zhang *et al*[108], with some modification. Slices were incubated in a medium (DM/KYN) containing (mM): 134 Na-isethionate, 23 glucose, 2 KCl, 4 $MgCl_2$, 1 $CaCl_2$, 1 kynurenic

acid, 15 HEPES, and supplemented with 0.75 mg/ml protease type XIV (Sigma P-5147). Enzymatic treatment was carried out at 37°C, for a time proportional to mice age (from 19 min for P13, to 24 min for P18). After rinsing with DM/KYN, the VTA region was cut out with a polished needle under a stereomicroscope and laid on a Petri dish pretreated with concanavalin A (50 µg/ml). After delicate mechanical dissociation with a fire-polished micro-Pasteur pipette, cells were left at 30 °C in a humidified chamber, for at least 30 min. DA cells were identified by their slow spontaneous discharge frequency (2-3 Hz on average[23,109] and the rapid blockade of cell firing by 100 µM DA, which activates inward rectifying K^+ channels by engaging D_2 autoreceptors[110]. Applying DA before or after testing the OX response did not alter cellular response, thus ruling out potential cross talk between D_2Rs and OXRs. Patch-clamp recordings were carried out in cell-attached configuration at room temperature using an Axopatch 200B amplifier (Molecular Devices). Signals were low-pass filtered at 2 kHz and digitized at 10 kHz, with pClamp9/Digidata 1322A (Molecular Devices). During the experiments, neurons were perfused with an extracellular solution containing (mM): 145 NaCl, 1 $MgCl_2$, 3.5 KCl, 2 CaCl2, 5 glucose, 10 HEPES (pH 7.25). The pipette contained (mM): 140 K-gluconate, 10 NaCl, 1 $MgCl_2$, 2 MgATP, 0.3 NaGTP, 0.1 BAPTA, 10 HEPES (pH 7.3). Drugs were applied with an RSC-160 Rapid Solution Changer (BioLogic Science Instruments).

Patch-clamp electrophysiological recordings of DA neurons in VTA brain slices

Mice (10- to 13-week-old) were anaesthetized with isoflurane and decapitated. The brain was quickly removed and coronal slices (200 µm-thick) containing the midbrain were prepared using a vibrating tissue slicer (Campden Instruments, Loughborough, UK) in oxygenated (95% O_2 / 5% CO_2) ice-cold modified artificial cerebrospinal fluid (aCSF) containing (in mM): 105 sucrose, 65 NaCl, 25 $NaHCO_3$, 2.5 KCl, 1.25 NaH_2PO_4, 7 $MgCl_2$, 0.5 $CaCl_2$, 25 glucose, 1.7 L(+)-ascorbic acid. Slices recovered for 1 h at 35°C in standard aCSF containing (in mM): 130 NaCl, 25 $NaHCO_3$, 2.5 KCl, 1.25 NaH_2PO_4, 1.2 $MgCl_2$, 2 $CaCl_2$, 18 glucose, 1.7 L(+)-ascorbic acid, and complemented with 2 sodium pyruvate and 3 myo-inositol. In the recording chamber, slices were superfused with oxygenated standard aCSF at nearly physiological temperature (30-32°C). In all patch-clamp recordings of DA cells from VTA slices, we targeted lateral VTA cells, reported to project to the lateral NAc-shell, based on their location and presence of an I_h current[46]. Neurons were patched in the whole-cell configuration with borosilicate glass pipettes (2-4 MΩ) filled with (in mM): 130 K-gluconate, 10 KCl, 10 HEPES, 10 Na-phosphocreatine, 0.2 EGTA, 4 Mg-ATP, 0.2 Na-GTP, (290-300 mOsm, pH 7.2-7.3). Recorded neurons were considered dopaminergic if they exhibited an inward current/sag in response to hyperpolarizing voltage/current steps, as well as a >3 mV hyperpolarization upon perfusion of the $GABA_BR$ agonist baclofen (1 µM) at the end of the recording[111]. To assess basal intrinsic excitability, cell firing was first elicited by providing 1-s long incremental somatic current injections while the membrane potential was held at -60 mV. To study the effect of OXA and OXB on intrinsic excitability, we used a protocol previously described[46]. Briefly, neuronal firing was elicited by a depolarizing current injection of 500 ms duration and of constant amplitude. Following a baseline period of 10 min, 100 nM OXA or OXB was bath-applied for 5 min. Throughout these recordings, cells were held at -60 mV by direct current injection, in order to minimize the contribution of synaptic depolarization/hyperpolarization and isolate the effect of orexin peptides on intrinsic excitability. Baimel *et al*[46] demonstrated that the effect of OXA is independent of synaptic transmission. We also verified that the effect of OXB on DA^{VTA} cells

persists in the presence of synaptic blockers (**Fig. 7h-i**) (100 µM picrotoxin, 10 µM DNQX and 50 µM D,L-APV, to antagonize $GABA_A$Rs, AMPARs and NMDARs, respectively).

Recordings in the current-clamp configuration were conducted with bridge balance. Membrane voltage values were not corrected for liquid junction potential. Data were acquired through a Digidata1550A digitizer. Signals were amplified through a Multiclamp700B amplifier (Molecular Devices, Sunnyvale, USA), sampled at 20 kHz and filtered at 10 kHz using Clampex10 (Molecular Devices). Clampfit10 (Molecular Devices) was used for data analysis.

Statistics

The data were analysed by independent samples *t*-tests, paired samples *t*-tests and repeated measures ANOVA, as appropriate, using the statistical packages SPSS (Chicago, IL, USA), GraphPad Prism (San Diego, CA, USA), or OriginPro 2023 (OriginLab Corporation). Shapiro-Wilk analysis was used to assess the normality of sample distribution. When normality was violated, non-parametric tests (Wilcoxon or Mann-Whitney, as appropriate) were applied as stated in figure legends. For repeated measures two-way ANOVA, *P* values of main effects and interaction are reported in the figure legends for each experiment. All bars and error bars represent mean ± S.E.M. Statistical significance was set at $P<0.05$, and *P*-value was considered trending toward significance when $0.05 \leqslant P \leqslant 0.1$.

DATA AVAILABILITY. The datasets acquired for this study are available from the corresponding author upon request.

CODE AVAILABILITY. Custom-written scripts for data analysis used in this study are available from the corresponding author upon request.

REFERENCES

1. de Lecea L, Kilduff TS, Peyron C, Gao X, Foye PE, Danielson PE *et al.* The hypocretins: hypothalamus-specific peptides with neuroexcitatory activity. *Proc Natl Acad Sci U S A* 1998; **95**(1)**:** 322-327.

2. Sakurai T, Amemiya A, Ishii M, Matsuzaki I, Chemelli RM, Tanaka H *et al.* Orexins and orexin receptors: a family of hypothalamic neuropeptides and G protein-coupled receptors that regulate feeding behavior. *Cell* 1998; **92**(5)**:** 1 page following 696.

3. Peyron C, Tighe DK, van den Pol AN, de Lecea L, Heller HC, Sutcliffe JG *et al.* Neurons containing hypocretin (orexin) project to multiple neuronal systems. *J Neurosci* 1998; **18**(23)**:** 9996-10015.

4. Li SB, Damonte VM, Chen C, Wang GX, Kebschull JM, Yamaguchi H *et al.* Hyperexcitable arousal circuits drive sleep instability during aging. *Science* 2022; **375**(6583)**:** eabh3021.

5. Lee MG, Hassani OK, Jones BE. Discharge of identified orexin/hypocretin neurons across the sleep-waking cycle. *J Neurosci* 2005; **25**(28)**:** 6716-6720.

6. Adamantidis AR, Zhang F, Aravanis AM, Deisseroth K, de Lecea L. Neural substrates of awakening probed with optogenetic control of hypocretin neurons. *Nature* 2007; **450**(7168)**:** 420-424.

7. Broglia G, Corsi G, Bouvier P-HP, Vassalli A, Tafti M, Bandarabadi M. Hypothalamic control of noradrenergic neurons stabilizes sleep. *bioRxiv* 2024.

8. Mochizuki T, Crocker A, McCormack S, Yanagisawa M, Sakurai T, Scammell TE. Behavioral state instability in orexin knock-out mice. *J Neurosci* 2004; **24**(28)**:** 6291-6300.

9. Vassalli A, Franken P. Hypocretin (orexin) is critical in sustaining theta/gamma-rich waking behaviors that drive sleep need. *Proc Natl Acad Sci U S A* 2017; **114**(27)**:** E5464-E5473.

10. Liblau RS, Vassalli A, Seifinejad A, Tafti M. Hypocretin (orexin) biology and the pathophysiology of narcolepsy with cataplexy. *Lancet Neurol* 2015; **14**(3)**:** 318-328.

11. Scammell TE, Winrow CJ. Orexin receptors: pharmacology and therapeutic opportunities. *Annu Rev Pharmacol Toxicol* 2011; **51:** 243-266.

12. Seifinejad A, Vassalli A, Tafti M. Neurobiology of cataplexy. *Sleep Med Rev* 2021; **60:** 101546.

13. Eban-Rothschild A, Appelbaum L, de Lecea L. Neuronal Mechanisms for Sleep/Wake Regulation and Modulatory Drive. *Neuropsychopharmacology* 2018; **43**(5)**:** 937-952.

14. Villano I, Messina A, Valenzano A, Moscatelli F, Esposito T, Monda V *et al.* Basal Forebrain Cholinergic System and Orexin Neurons: Effects on Attention. *Front Behav Neurosci* 2017; **11:** 10.

15. Burgess CR, Scammell TE. Narcolepsy: neural mechanisms of sleepiness and cataplexy. *J Neurosci* 2012; **32**(36)**:** 12305-12311.

16. Okura M, Fujiki N, Kita I, Honda K, Yoshida Y, Mignot E *et al.* The roles of midbrain and diencephalic dopamine cell groups in the regulation of cataplexy in narcoleptic Dobermans. *Neurobiol Dis* 2004; **16**(1)**:** 274-282.

17. Lammel S, Ion DI, Roeper J, Malenka RC. Projection-specific modulation of dopamine neuron synapses by aversive and rewarding stimuli. *Neuron* 2011; **70**(5)**:** 855-862.

18. Groenewegen HJ, Wright CI, Beijer AV, Voorn P. Convergence and segregation of ventral striatal inputs and outputs. *Ann N Y Acad Sci* 1999; **877:** 49-63.

19. Bandarabadi M, Li S, Aeschlimann L, Colombo G, Tzanoulinou S, Tafti M *et al.* Inactivation of hypocretin receptor-2 signaling in dopaminergic neurons induces hyperarousal and enhanced cognition but impaired inhibitory control. *Mol Psychiatry* 2023.

20. Mohammadkhani A, Mitchell C, James MH, Borgland SL, Dayas CV. Contribution of hypothalamic orexin (hypocretin) circuits to pathologies of motivation. *Br J Pharmacol* 2024; **181**(22)**:** 4430-4449.

21. Calipari ES, Espana RA. Hypocretin/orexin regulation of dopamine signaling: implications for reward and reinforcement mechanisms. *Front Behav Neurosci* 2012; **6:** 54.

22. James MH, Aston-Jones G. Orexin Reserve: A Mechanistic Framework for the Role of Orexins (Hypocretins) in Addiction. *Biol Psychiatry* 2022; **92**(11)**:** 836-844.

23. Korotkova TM, Sergeeva OA, Eriksson KS, Haas HL, Brown RE. Excitation of ventral tegmental area dopaminergic and nondopaminergic neurons by orexins/hypocretins. *J Neurosci* 2003; **23**(1)**:** 7-11.

24. Nakamura T, Uramura K, Nambu T, Yada T, Goto K, Yanagisawa M *et al.* Orexin-induced hyperlocomotion and stereotypy are mediated by the dopaminergic system. *Brain Res* 2000; **873**(1)**:** 181-187.

25. Borgland SL, Taha SA, Sarti F, Fields HL, Bonci A. Orexin A in the VTA is critical for the induction of synaptic plasticity and behavioral sensitization to cocaine. *Neuron* 2006; **49**(4)**:** 589-601.

26. Borgland SL, Storm E, Bonci A. Orexin B/hypocretin 2 increases glutamatergic transmission to ventral tegmental area neurons. *Eur J Neurosci* 2008; **28**(8)**:** 1545-1556.

27. Thomas CS, Mohammadkhani A, Rana M, Qiao M, Baimel C, Borgland SL. Optogenetic stimulation of lateral hypothalamic orexin/dynorphin inputs in the ventral tegmental area potentiates mesolimbic dopamine neurotransmission and promotes reward-seeking behaviours. *Neuropsychopharmacology* 2022; **47**(3)**:** 728-740.

28. Williams JT, Bolli MH, Brotschi C, Sifferlen T, Steiner MA, Treiber A *et al.* Discovery of Nivasorexant (ACT-539313): The First Selective Orexin-1 Receptor Antagonist (SO1RA) Investigated in Clinical Trials. *J Med Chem* 2024; **67**(4)**:** 2337-2348.

29. Korotkova TM, Eriksson KS, Haas HL, Brown RE. Selective excitation of GABAergic neurons in the substantia nigra of the rat by orexin/hypocretin in vitro. *Regul Pept* 2002; **104**(1-3)**:** 83-89.

30. Fenwick EM, Marty A, Neher E. A patch-clamp study of bovine chromaffin cells and of their sensitivity to acetylcholine. *J Physiol* 1982; **331:** 577-597.

31. Asahi S, Egashira S, Matsuda M, Iwaasa H, Kanatani A, Ohkubo M *et al.* Development of an orexin-2 receptor selective agonist, [Ala(11), D-Leu(15)]orexin-B. *Bioorg Med Chem Lett* 2003; **13**(1)**:** 111-113.

32. Simon P, Dupuis R, Costentin J. Thigmotaxis as an index of anxiety in mice. Influence of dopaminergic transmissions. *Behav Brain Res* 1994; **61**(1)**:** 59-64.

33. Blomeley C, Garau C, Burdakov D. Accumbal D2 cells orchestrate innate risk-avoidance according to orexin signals. *Nat Neurosci* 2017.

34. File SE, Mabbutt PS, Hitchcott PK. Characterisation of the phenomenon of "one-trial tolerance" to the anxiolytic effect of chlordiazepoxide in the elevated plus-maze. *Psychopharmacology (Berl)* 1990; **102**(1)**:** 98-101.

35. Treit D, Menard J, Royan C. Anxiogenic stimuli in the elevated plus-maze. *Pharmacol Biochem Behav* 1993; **44**(2)**:** 463-469.

36. Zhou H, Yu CL, Wang LP, Yang YX, Mao RR, Zhou QX *et al.* NMDA and D1 receptors are involved in one-trial tolerance to the anxiolytic-like effects of diazepam in the elevated plus maze test in rats. *Pharmacol Biochem Behav* 2015; **135:** 40-45.

37. Frussa-Filho R, Ribeiro Rde A. One-trial tolerance to the effects of chlordiazepoxide in the elevated plus-maze is not due to acquisition of a phobic avoidance of open arms during initial exposure. *Life Sci* 2002; **71**(5)**:** 519-525.

38. File SE, Zangrossi H, Jr., Viana M, Graeff FG. Trial 2 in the elevated plus-maze: a different form of fear? *Psychopharmacology (Berl)* 1993; **111**(4)**:** 491-494.

39. Bariselli S, Glangetas C, Tzanoulinou S, Bellone C. Ventral tegmental area subcircuits process rewarding and aversive experiences. *J Neurochem* 2016; **139**(6)**:** 1071-1080.

40. Solie C, Girard B, Righetti B, Tapparel M, Bellone C. VTA dopamine neuron activity encodes social interaction and promotes reinforcement learning through social prediction error. *Nat Neurosci* 2022; **25**(1)**:** 86-97.

41. Gunaydin LA, Deisseroth K. Dopaminergic Dynamics Contributing to Social Behavior. *Cold Spring Harb Symp Quant Biol* 2014; **79:** 221-227.

42. Dawson M, Terstege DJ, Jamani N, Tsutsui M, Pavlov D, Bugescu R *et al.* Hypocretin/orexin neurons encode social discrimination and exhibit a sex-dependent necessity for social interaction. *Cell Rep* 2023; **42**(7)**:** 112815.

43. Abbas MG, Shoji H, Soya S, Hondo M, Miyakawa T, Sakurai T. Comprehensive Behavioral Analysis of Male Ox1r (-/-) Mice Showed Implication of Orexin Receptor-1 in Mood, Anxiety, and Social Behavior. *Front Behav Neurosci* 2015; **9:** 324.

44. Moy SS, Nadler JJ, Perez A, Barbaro RP, Johns JM, Magnuson TR *et al.* Sociability and preference for social novelty in five inbred strains: an approach to assess autistic-like behavior in mice. *Genes Brain Behav* 2004; **3**(5)**:** 287-302.

45. Bari A, Dalley JW, Robbins TW. The application of the 5-choice serial reaction time task for the assessment of visual attentional processes and impulse control in rats. *Nat Protoc* 2008; **3**(5)**:** 759-767.

46. Baimel C, Lau BK, Qiao M, Borgland SL. Projection-Target-Defined Effects of Orexin and Dynorphin on VTA Dopamine Neurons. *Cell Reports* 2017; **18**(6)**:** 1346-1355.

47. Peleg-Raibstein D, Burdakov D. Do orexin/hypocretin neurons signal stress or reward? *Peptides* 2021; **145:** 170629.

48. Schultz W, Dayan P, Montague PR. A neural substrate of prediction and reward. *Science* 1997; **275**(5306)**:** 1593-1599.

49. Flagel SB, Clark JJ, Robinson TE, Mayo L, Czuj A, Willuhn I *et al.* A selective role for dopamine in stimulus-reward learning. *Nature* 2011; **469**(7328)**:** 53-57.

50. Berke JD. What does dopamine mean? *Nat Neurosci* 2018; **21**(6)**:** 787-793.

51. Cryan JF, Holmes A. The ascent of mouse: advances in modelling human depression and anxiety. *Nat Rev Drug Discov* 2005; **4**(9)**:** 775-790.

52. McGraw M, Christensen C, Nelson H, Li AJ, Qualls-Creekmore E. Divergent changes in social stress-induced motivation in male and female mice. *Physiol Behav* 2025; **291:** 114787.

53. Figueiredo Cerqueira MM, Castro MML, Vieira AA, Kurosawa JAA, Amaral Junior FLD, Siqueira Mendes FCC *et al.* Comparative analysis between Open Field and Elevated Plus Maze tests as a method for evaluating anxiety-like behavior in mice. *Heliyon* 2023; **9**(4)**:** e14522.

54. Xiao X, Yeghiazaryan G, Cremer AL, Backes H, Kloppenburg P, Hausen AC. Deficiency of Orexin Receptor Type 1 in Dopaminergic Neurons Increases Novelty-Induced Locomotion and Exploration. 2023.

55. Ekstrand MI, Terzioglu M, Galter D, Zhu S, Hofstetter C, Lindqvist E *et al.* Progressive parkinsonism in mice with respiratory-chain-deficient dopamine neurons. *Proc Natl Acad Sci U S A* 2007; **104**(4)**:** 1325-1330.

56. Backman CM, Malik N, Zhang Y, Shan L, Grinberg A, Hoffer BJ *et al.* Characterization of a mouse strain expressing Cre recombinase from the 3' untranslated region of the dopamine transporter locus. *Genesis* 2006; **44**(8)**:** 383-390.

57. Giros B, Jaber M, Jones SR, Wightman RM, Caron MG. Hyperlocomotion and indifference to cocaine and amphetamine in mice lacking the dopamine transporter. *Nature* 1996; **379**(6566)**:** 606-612.

58. Costa KM, Schenkel D, Roeper J. Sex-dependent alterations in behavior, drug responses and dopamine transporter expression in heterozygous DAT-Cre mice. *Sci Rep* 2021; **11**(1)**:** 3334.

59. Li S, Franken P, Vassalli A. Bidirectional and context-dependent changes in theta and gamma oscillatory brain activity in noradrenergic cell-specific Hypocretin/Orexin receptor 1-KO mice. *Scientific Reports* 2018; **8**(1)**:** 15474.

60. Zalocusky KA, Ramakrishnan C, Lerner TN, Davidson TJ, Knutson B, Deisseroth K. Nucleus accumbens D2R cells signal prior outcomes and control risky decision-making. *Nature* 2016; **531**(7596)**:** 642-646.

61. van den Pol AN, Gao XB, Obrietan K, Kilduff TS, Belousov AB. Presynaptic and postsynaptic actions and modulation of neuroendocrine neurons by a new hypothalamic peptide, Hypocretin/Orexin. *Journal of Neuroscience* 1998; **18**(19)**:** 7962-7971.

62. Patyal R, Woo EY, Borgland SL. Local hypocretin-1 modulates terminal dopamine concentration in the nucleus accumbens shell. *Front Behav Neurosci* 2012; **6:** 82.

63. Lambe EK, Aghajanian GK. Hypocretin (orexin) induces calcium transients in single spines postsynaptic to identified thalamocortical boutons in prefrontal slice. *Neuron* 2003; **40**(1)**:** 139-150.

64. Aracri P, Banfi D, Pasini ME, Amadeo A, Becchetti A. Hypocretin (orexin) regulates glutamate input to fast-spiking interneurons in layer V of the Fr2 region of the murine prefrontal cortex. *Cereb Cortex* 2015; **25**(5)**:** 1330-1347.

65. Kroener S, Chandler LJ, Phillips PE, Seamans JK. Dopamine modulates persistent synaptic activity and enhances the signal-to-noise ratio in the prefrontal cortex. *PLoS One* 2009; **4**(8)**:** e6507.

66. Ott T, Nieder A. Dopamine and Cognitive Control in Prefrontal Cortex. *Trends Cogn Sci* 2019; **23**(3)**:** 213-234.

67. Stalter M, Westendorff S, Nieder A. Dopamine Gates Visual Signals in Monkey Prefrontal Cortex Neurons. *Cell Rep* 2020; **30**(1)**:** 164-172 e164.

68. Salamone JD, Correa M. The Neurobiology of Activational Aspects of Motivation: Exertion of Effort, Effort-Based Decision Making, and the Role of Dopamine. *Annu Rev Psychol* 2024; **75:** 1-32.

69. Zweifel LS, Fadok JP, Argilli E, Garelick MG, Jones GL, Dickerson TM *et al.* Activation of dopamine neurons is critical for aversive conditioning and prevention of generalized anxiety. *Nat Neurosci* 2011; **14**(5)**:** 620-626.

70. Stelly CE, Haug GC, Fonzi KM, Garcia MA, Tritley SC, Magnon AP *et al.* Pattern of dopamine signaling during aversive events predicts active avoidance learning. *Proc Natl Acad Sci U S A* 2019; **116**(27)**:** 13641-13650.

71. Zeidler Z, Gomez MF, Gupta TA, Shari M, Wilke SA, DeNardo LA. Prefrontal dopamine activity is critical for rapid threat avoidance learning. *bioRxiv* 2025.

72. Tzanoulinou S, Musardo S, Contestabile A, Bariselli S, Casarotto G, Magrinelli E *et al.* Inhibition of Trpv4 rescues circuit and social deficits unmasked by acute inflammatory response in a Shank3 mouse model of Autism. *Mol Psychiatry* 2022; **27**(4)**:** 2080-2094.

73. Contestabile A, Casarotto G, Girard B, Tzanoulinou S, Bellone C. Deconstructing the contribution of sensory cues in social approach. *Eur J Neurosci* 2021; **53**(9)**:** 3199-3211.

74. Crawley JN. Designing mouse behavioral tasks relevant to autistic-like behaviors. *Ment Retard Dev Disabil Res Rev* 2004; **10**(4)**:** 248-258.

75. Silverman JL, Thurm A, Ethridge SB, Soller MM, Petkova SP, Abel T *et al.* Reconsidering animal models used to study autism spectrum disorder: Current state and optimizing future. *Genes Brain Behav* 2022; **21**(5)**:** e12803.

76. Genovese A, Butler MG. The Autism Spectrum: Behavioral, Psychiatric and Genetic Associations. *Genes (Basel)* 2023; **14**(3).

77. Sato M, Nakai N, Fujima S, Choe KY, Takumi T. Social circuits and their dysfunction in autism spectrum disorder. *Mol Psychiatry* 2023; **28**(8)**:** 3194-3206.

78. Willie JT, Chemelli RM, Sinton CM, Tokita S, Williams SC, Kisanuki YY *et al.* Distinct narcolepsy syndromes in Orexin receptor-2 and Orexin null mice: molecular genetic dissection of Non-REM and REM sleep regulatory processes. *Neuron* 2003; **38**(5)**:** 715-730.

79. Kukkonen JP, Turunen PM. Cellular Signaling Mechanisms of Hypocretin/Orexin. *Front Neurol Neurosci* 2021; **45:** 91-102.

80. Muroya S, Funahashi H, Yamanaka A, Kohno D, Uramura K, Nambu T *et al.* Orexins (hypocretins) directly interact with neuropeptide Y, POMC and glucose-responsive neurons to regulate Ca 2+ signaling in a reciprocal manner to leptin: orexigenic neuronal pathways in the mediobasal hypothalamus. *Eur J Neurosci* 2004; **19**(6)**:** 1524-1534.

81. Ma X, Zubcevic L, Bruning JC, Ashcroft FM, Burdakov D. Electrical inhibition of identified anorexigenic POMC neurons by orexin/hypocretin. *J Neurosci* 2007; **27**(7)**:** 1529-1533.

82. Belle MD, Hughes AT, Bechtold DA, Cunningham P, Pierucci M, Burdakov D *et al.* Acute suppressive and long-term phase modulation actions of orexin on the mammalian circadian clock. *J Neurosci* 2014; **34**(10)**:** 3607-3621.

83. Izawa S, Fusca D, Jiang H, Heilinger C, Hausen AC, Wunderlich FT *et al.* Orexin/hypocretin receptor 2 signaling in MCH neurons regulates REM sleep and insulin sensitivity. *Cell Rep* 2025; **44**(2)**:** 115277.

84. Ishibashi M, Gumenchuk I, Miyazaki K, Inoue T, Ross WN, Leonard CS. Hypocretin/Orexin Peptides Alter Spike Encoding by Serotonergic Dorsal Raphe Neurons through Two Distinct Mechanisms That Increase the Late Afterhyperpolarization. *J Neurosci* 2016; **36**(39)**:** 10097-10115.

85. Um KB, Kwak S, Cheon SH, Kim J, Hwang SK. AST-001 Improves Social Deficits and Restores Dopamine Neuron Activity in a Mouse Model of Autism. *Biomedicines* 2023; **11**(12).

86. Leger L, Sapin E, Goutagny R, Peyron C, Salvert D, Fort P *et al.* Dopaminergic neurons expressing Fos during waking and paradoxical sleep in the rat. *J Chem Neuroanat* 2010; **39**(4)**:** 262-271.

87. Cho JR, Treweek JB, Robinson JE, Xiao C, Bremner LR, Greenbaum A *et al.* Dorsal Raphe Dopamine Neurons Modulate Arousal and Promote Wakefulness by Salient Stimuli. *Neuron* 2017; **94**(6)**:** 1205-1219 e1208.

88. Korchynska S, Rebernik P, Pende M, Boi L, Alpar A, Tasan R *et al.* A hypothalamic dopamine locus for psychostimulant-induced hyperlocomotion in mice. *Nat Commun* 2022; **13**(1)**:** 5944.

89. Liu C, Xue Y, Liu MF, Wang Y, Liu ZR, Diao HL *et al.* Orexins increase the firing activity of nigral dopaminergic neurons and participate in motor control in rats. *J Neurochem* 2018; **147**(3)**:** 380-394.

90. Bian K, Liu C, Wang Y, Xue Y, Chen L. Orexin-B exerts excitatory effects on nigral dopaminergic neurons and alleviates motor disorders in MPTP parkinsonian mice. *Neurosci Lett* 2021; **765:** 136291.

91. Reid MS, Tafti M, Nishino S, Sampathkumaran R, Siegel JM, Mignot E. Local administration of dopaminergic drugs into the ventral tegmental area modulates cataplexy in the narcoleptic canine. *Brain Res* 1996; **733**(1)**:** 83-100.

92. Dauvilliers Y, Mignot E, Del Rio Villegas R, Du Y, Hanson E, Inoue Y *et al.* Oral Orexin Receptor 2 Agonist in Narcolepsy Type 1. *N Engl J Med* 2023; **389**(4)**:** 309-321.

93. Oishi Y, Williams RH, Agostinelli L, Arrigoni E, Fuller PM, Mochizuki T *et al.* Role of the medial prefrontal cortex in cataplexy. *J Neurosci* 2013; **33**(23)**:** 9743-9751.

94. Vassalli A, Dellepiane JM, Emmenegger Y, Jimenez S, Vandi S, Plazzi G *et al.* Electroencephalogram paroxysmal theta characterizes cataplexy in mice and children. *Brain* 2013; **136**(Pt 5)**:** 1592-1608.

95. Jacobson LH, Hoyer D, de Lecea L. Hypocretins (orexins): The ultimate translational neuropeptides. *J Intern Med* 2022; **291**(5)**:** 533-556.

96. McGregor R, Wu MF, Thannickal TC, Siegel JM. Opiate anticipation, opiate induced anatomical changes in hypocretin (Hcrt, orexin) neurons and opiate induced microglial activation are blocked by the dual Hcrt receptor antagonist suvorexant, while opiate analgesia is maintained. *bioRxiv* 2024.

97. Tzanoulinou S, Riccio O, de Boer MW, Sandi C. Peripubertal stress-induced behavioral changes are associated with altered expression of genes involved in excitation and inhibition in the amygdala. *Transl Psychiatry* 2014; **4**(7)**:** e410.

98. Walf AA, Frye CA. The use of the elevated plus maze as an assay of anxiety-related behavior in rodents. *Nat Protoc* 2007; **2**(2)**:** 322-328.

99. Sasamori H, Ohmura Y, Kubo T, Yoshida T, Yoshioka M. Assessment of impulsivity in adolescent mice: A new training procedure for a 3-choice serial reaction time task. *Behav Brain Res* 2018; **343:** 61-70.

100. Asinof SK, Paine TA. The 5-choice serial reaction time task: a task of attention and impulse control for rodents. *J Vis Exp* 2014; (90)**:** e51574.

101. Tsutsui-Kimura I, Ohmura Y, Izumi T, Yamaguchi T, Yoshida T, Yoshioka M. The effects of serotonin and/or noradrenaline reuptake inhibitors on impulsive-like action assessed by the three-choice serial reaction time task: a simple and valid model of impulsive action using rats. *Behav Pharmacol* 2009; **20**(5-6)**:** 474-483.

102. Humby T, Wilkinson L, Dawson G. Assaying aspects of attention and impulse control in mice using the 5-choice serial reaction time task. *Curr Protoc Neurosci* 2005; **Chapter 8:** Unit 8 5H.

103. Cain CK. Avoidance Problems Reconsidered. *Curr Opin Behav Sci* 2019; **26:** 9-17.

104. Tabibnia G. An affective neuroscience model of boosting resilience in adults. *Neurosci Biobehav Rev* 2020; **115:** 321-350.

105. Diehl MM, Bravo-Rivera C, Quirk GJ. The study of active avoidance: A platform for discussion. *Neurosci Biobehav Rev* 2019; **107:** 229-237.

106. Meneghini S, Modena D, Colombo G, Coatti A, Milani N, Madaschi L *et al.* The beta2(V287L) nicotinic subunit linked to sleep-related epilepsy differently affects fast-spiking and regular spiking somatostatin-expressing neurons in murine prefrontal cortex. *Prog Neurobiol* 2022; **214:** 102279.

107. Franklin KBJ, Paxinos G. *Paxinos and Franklin's The mouse brain in stereotaxic coordinates*. Fourth edition. edn, 1 volume (unpaged)pp.

108. Zhang HY, Gao M, Shen H, Bi GH, Yang HJ, Liu QR *et al.* Expression of functional cannabinoid CB(2) receptor in VTA dopamine neurons in rats. *Addict Biol* 2017; **22**(3)**:** 752-765.

109. Khaliq ZM, Bean BP. Pacemaking in dopaminergic ventral tegmental area neurons: depolarizing drive from background and voltage-dependent sodium conductances. *J Neurosci* 2010; **30**(21)**:** 7401-7413.

110. Ford CP. The role of D2-autoreceptors in regulating dopamine neuron activity and transmission. *Neuroscience* 2014; **282:** 13-22.

111. Margolis EB, Toy B, Himmels P, Morales M, Fields HL. Identification of rat ventral tegmental area GABAergic neurons. *PLoS One* 2012; **7**(7)**:** e42365.

ACKNOWLEDGMENTS. This work was supported by the Swiss National Science Foundation (grant 31003A_182613 to AV), and by the University of Milano-Bicocca (post-doctoral fellowship to LCG, 2021-ATE-0042 and 2024-ATE-0117 to AB). We thank Anne-Catherine Thomas for animal genotyping.

AUTHOR CONTRIBUTIONS. ST conceived, performed and analyzed behavioral experiments with experimental help of RK and SR for the 3-CSRTT; SA conceived, performed and analyzed patch clamp recordings of cells in brain slices; LCG, FG, and AB conceived, performed and analyzed patch clamp recordings of dissociated dopamine neurons; AV generated the mouse lines; AV, AB, and MT conceived and supervised the project. All authors contributed to manuscript writing and Figure design.

COMPETING INTERESTS. Authors declare no competing interests.

SUPPLEMENTARY INFORMATION.

- Figures S1 to S3
- Table S1

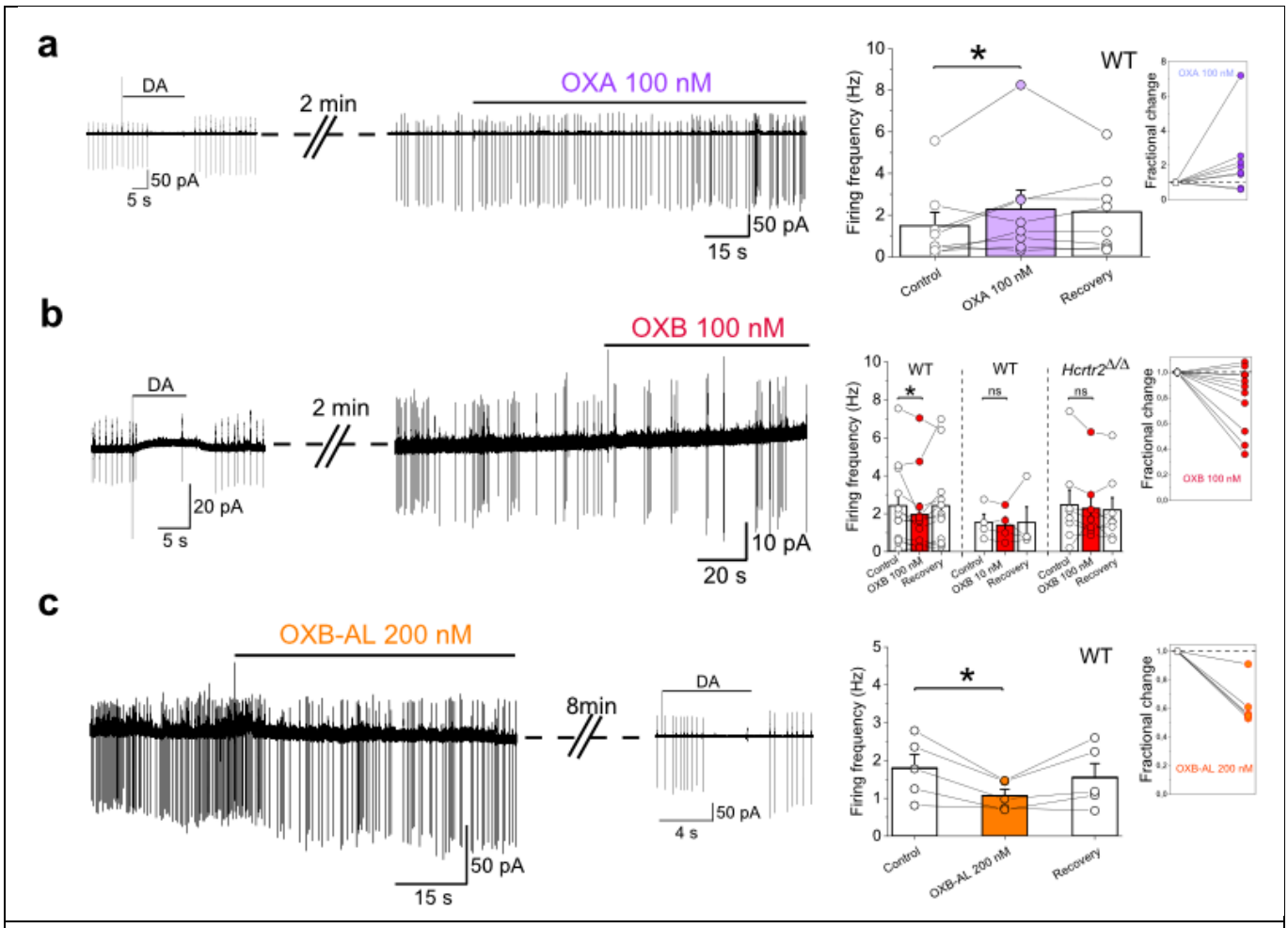

Fig. 1 OXA increases, whereas OXB decreases, cell firing of dissociated DA^{VTA} cells from C57BL/6J (WT) mice. Modulation of spontaneous electrophysiological activity of isolated dopamine neurons by orexin peptides. Action currents of dopamine cells acutely isolated from VTA slices of WT or *Hcrtr2*$^{\Delta/\Delta}$ (OX2R-deficient) mice were recorded by patch-clamping in cell-attached mode, in presence or absence of OXA (100 nM), OXB (10 or 100 nM), or the OX_2R-specific agonist OXB-AL (200 nM). $V_{pipette}$ was set to 0 mV.

(a) (*Left*) Representative trace showing spontaneous firing of a WT DA cell exposed to DA and next to OXA. (*Right*). Firing frequencies calculated before (Control; 2 min), during the second min of OXA exposure (Purple), or after washout (Recovery). Bar graphs: Control: 1.479 ± 0.64 Hz; OXA: 2.283 ± 0.91 Hz; Recovery: 2.149 ± 0.68 Hz (*P* = 0.042 between Control and OXA, paired *t*-test, n = 8). *(Inset)* Relative effect of OXA on firing activity of individual WT DA cells. Datapoints (Purple) are quotients of OXA and Control firing frequencies, for each cell. The Control values were set to 1.

(b) *(Left)*. Representative trace showing spontaneous firing of a WT DA cell exposed to DA, and next to OXB. (*Right*). Firing frequencies calculated for 2 min before (Control), during the first min of OXB exposure (Red), or after washout (Recovery). Left bar graphs (WT): Control: 2.42 ± 0.63 Hz; OXB 100 nM: 1.955 ± 0.59 Hz (*P* = 0.026; paired *t*-test; n = 12); Recovery: 2.42 ± 0.64 Hz. Middle bar graphs (WT): Control: 1.54 ± 0.44 Hz; OXB 10 nM: 1.39 ± 0.43 Hz (*P* = 0.102; paired *t*-test; n = 4); Recovery: 1.54 ± 0.81 Hz. Right bar graphs (*Hcrtr2*$^{\Delta/\Delta}$) depict data recorded from DA neurons isolated from VTA slices from mice lacking OX_2R in all cells[19]: Control 2.46 ± 0.79 Hz; OXB 100 nM: 2.28 ± 0.62 Hz (*P* = 0.255;

paired *t*-test; n = 8); Recovery: 2.195 ± 0.65 Hz. (Inset) Relative effect of OXB 100 nM (Red) on firing activity of individual WT DA cells, calculated as in (a).

(c) (*Left*) Representative trace showing spontaneous firing of WT DA cell exposed to OXB-AL, then to DA. (*Right*) Firing frequencies calculated for 2 min before (Control), during the first min of OXB-AL exposure (Orange), or after washout (Recovery). Bar graphs: Control: 1.8 ± 0.36 Hz; OXB-AL: 1.07 ± 0.17 Hz (P = 0.012; paired *t*-test; n = 5); Recovery: 1.55 ± 0.37 Hz. (*Inset*) Relative effect of OXB-AL (Orange) on firing activity of individual WT DA cells, calculated as in (a).

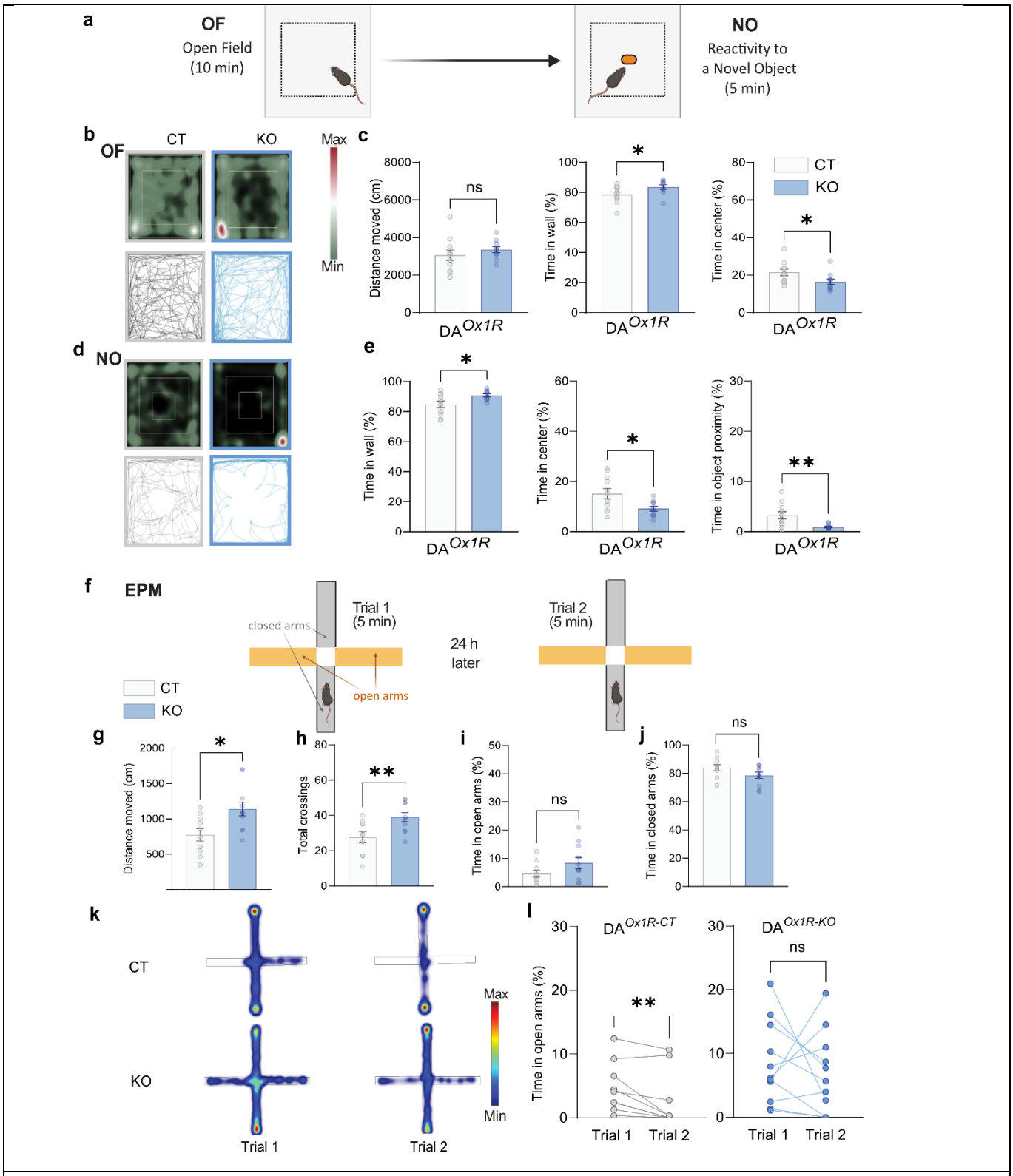

Fig. 2 Dopaminergic *Hcrtr1*-ablated mice show reduced exploration and reactivity to novelty in an open field, but hyperactivity and atypical responding in an elevated plus maze. DA$^{Ox1R\text{-}CT}$ and DA$^{Ox1R\text{-}KO}$ mice were subjected to the open field (OF), reactivity to novel object (NO) and elevated plus maze (EPM) tests. (**a**) Schematic design of the OF and NO tests conducted in a 34 x 34 (cm) ground floor-sized arena. Mice were allowed to freely explore the open field for 10 min (OF). Immediately afterward, an object

was placed in the arena center and mice allowed to freely explore the arena and the object for another 5 min (NO). The dashed-lined square delineates the center zone, defined as beyond ~x cm from the walls. (**b**) Heatmap (top) and trail map (bottom) of representative $DA^{Ox1R\text{-}CT}$ (left) and $DA^{Ox1R\text{-}KO}$ (right) mice during the 10 min OF exploration. Red and green indicate maximum and minimum occupancy, respectively. (**c**) (Left) Total distance traveled in the OF for $DA^{Ox1R\text{-}CT}$ and $DA^{Ox1R\text{-}KO}$ mice ($t(19) = 0.911$, $P = 0.370$, *t*-test); middle: time in the wall zone during OF ($t(19) = 2.183$, 0.042, *t*-test); (right) time in the center zone during OF (t (19) = 2.186, $P = 0.041$, *t*-test). (**d**) Heatmap (top) and trail map (bottom) of representative $DA^{Ox1R\text{-}CT}$ (left) and $DA^{Ox1R\text{-}KO}$ (right) mice during the 5 min reactivity to novel object test. (**e**) (Left) time in the wall zone during NO ($t(19) = 2.513$, $P = 0.021$, *t*-test); middle: time in the center zone during NO ($t(19) = 2.523$, $P = 0.021$, *t*-test); right: time in the center zone at 15 cm of the novel object ($t(19) = 3.039$, $P = 0.007$, *t*-test). n = 11 $DA^{Ox1R\text{-}CT}$, 10 $DA^{Ox1R\text{-}KO}$.
(**f**) Schematic design of the EPM test. Mice were subjected to an EPM trial for 5 min, and 24 h later were re-exposed to a 2nd EPM trial for another 5 min. (**g**) Distance moved during the 1st EPM trial revealed a higher total distance traveled by $DA^{Ox1R\text{-}KO}$ vs $DA^{Ox1R\text{-}CT}$ mice (t (19) = 2.777, $P = 0.012$, *t*-test), as well as (**h**) a higher total number of inter-zone crossings in KO vs CT (t (19) = 2.931, $P = 0.009$, *t*-test). (**i**) Time in the open arms (t (19) = 1.625, $P = 0.121$, *t*-test), and (**j**) Time in the closed arms (t (19) = 1.790, $P = 0.089$, t-test) were not significantly different in KO and CT. (**k**) Representative heatmaps depicting the location of a $DA^{Ox1R\text{-}CT}$ mouse (Top), and of a $DA^{Ox1R\text{-}KO}$ mouse during the 5-min EPM trials 1 and 2. (**l**) $DA^{Ox1R\text{-}CT}$ mice spend less time in open arms during the 2nd EPM trial than during the 1st, as commonly observed in rodents ($W = -51$, $P = 0.006$, Wilcoxon test). In contrast, $DA^{Ox1R\text{-}KO}$ mice do not spend less time in open arms during EPM Trial 2 relative to EPM Trial 1 (t (10) = 0.652, $P = 0.530$, paired *t*-test). Bar graphs depict mean ± SEM. n = 10 $DA^{Ox1R\text{-}CT}$, 11 $DA^{Ox1R\text{-}KO}$.

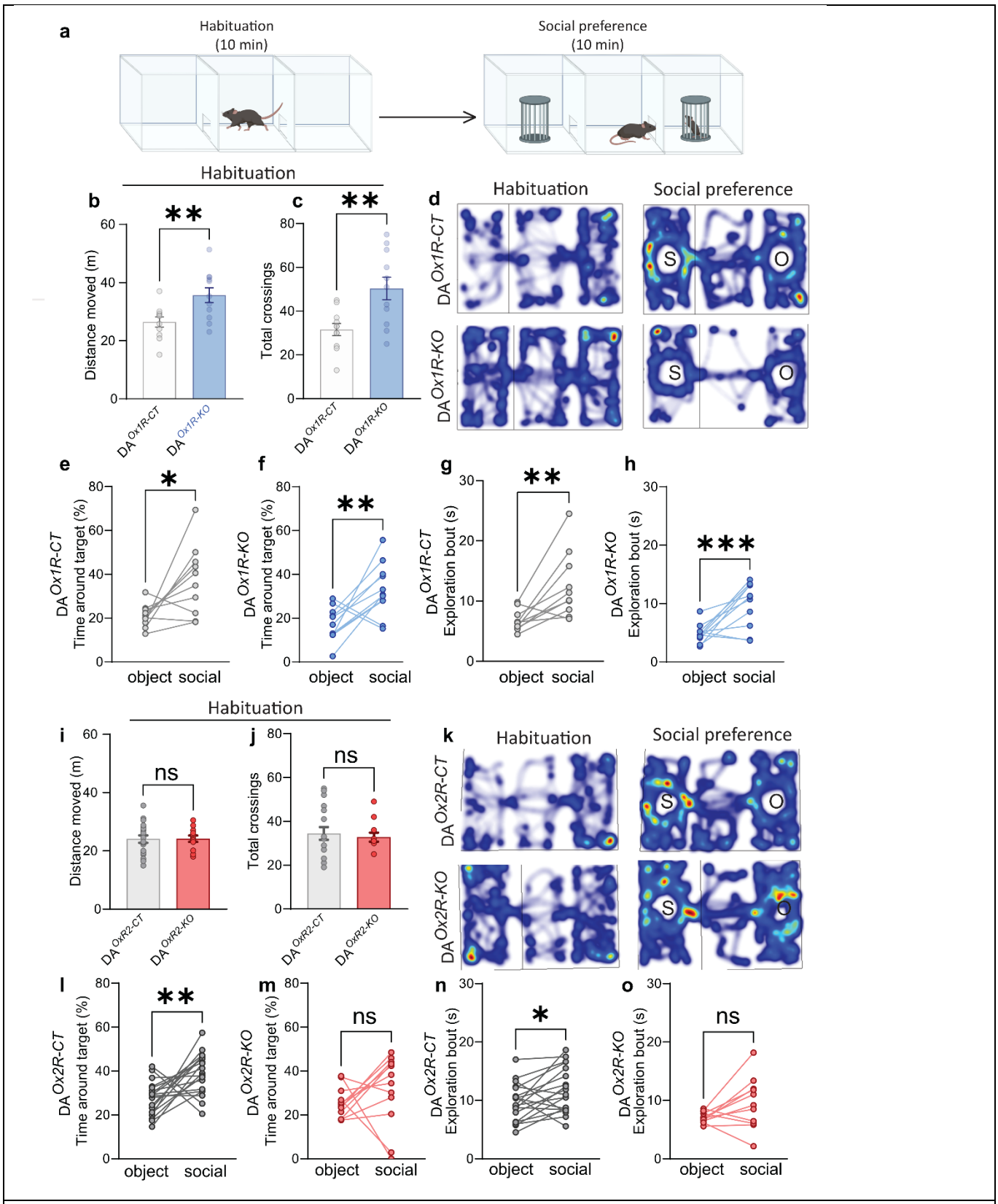

Fig. 3 Ablation of dopaminergic *Hcrtr2*, but not *Hcrtr1*, reduces sociability. The social preference of DA$^{Ox1R\text{-}KO}$ and DA$^{Ox2R\text{-}KO}$ mice was probed against their respective genetic controls using the 3-chamber test. (**a**) Schematic of the experimental design consisting of 2 phases (i) a 10 min-habituation phase, during which the mouse is allowed to freely explore the arena, and (ii) a directly subsequent 10 min-

social preference phase, during which 2 grided enclosures are located in the 2 opposite chambers, one empty and one containing a same-sex juvenile non-familiar mouse, and the experimental mouse is then allowed to freely explore the 3 chambers and interact with the juvenile using olfactory, visual, auditory, and tactile cues. During the habituation phase**,** $DA^{Ox1R\text{-}KO}$ mice were found to (**b**) travel across a longer total distance (t_{20} = 2.972, P = 0.007, t-test, n = 11 $DA^{Ox1R\text{-}CT}$, 11 $DA^{Ox1R\text{-}KO}$), and (**c**) perform a higher number of inter-zone crossings relative to $DA^{Ox1R\text{-}CT}$ mice (t_{20} = 3.224, P = 0.004, t-test, n = 11 $DA^{Ox1R\text{-}CT}$, 11 $DA^{Ox1R\text{-}KO}$). (**d**) Representative heatmaps of the location of a $DA^{Ox1R\text{-}CT}$ and a $DA^{Ox1R\text{-}KO}$ mouse during the habituation (left) and the social preference (right) phases. "S" denotes the social stimulus-containing enclosure, "O" denotes the object (empty) enclosure. Both $DA^{Ox1R\text{-}CT}$ (**e**) and $DA^{Ox1R\text{-}KO}$ (**f**) mice spent a higher % of total time within proximity to the social than the inanimate target ($DA^{Ox1R\text{-}CT}$: t (9) = 2.840, P = 0.019; $DA^{Ox1R\text{-}KO}$, t (10) = 3.230, P = 0.009; paired t-test). Both $DA^{Ox1R\text{-}CT}$ (**g**) and $DA^{Ox1R\text{-}KO}$ (**h**) mice displayed longer exploration bouts within proximity to the social than the inanimate target ($DA^{Ox1R\text{-}CT}$: t_9 = 3.564, P = 0.006; for $DA^{Ox1R\text{-}KO}$: t (10) = 3.987, P = 0.003; paired t-test). n = 10 $DA^{Ox1R\text{-}CT}$, 11 $DA^{Ox1R\text{-}KO}$).

In contrast to $DA^{Ox1R\text{-}KO}$ mice, during the habituation phase, $DA^{Ox2R\text{-}KO}$ mice did not exhibit any differences in total distance traveled (**i**), nor in total number of inter-chamber-crossings (**j**), compared to $DA^{Ox2R\text{-}CT}$ control mice (total distance moved: $DA^{Ox2R\text{-}CT}$ vs $DA^{Ox2R\text{-}KO}$, t (29) = 0.065, P = 0.949, t-test, n = 19 $DA^{Ox2R\text{-}CT}$, 12 $DA^{Ox2R\text{-}KO}$; total inter-chamber crossings: $DA^{Ox2R\text{-}CT}$ vs $DA^{Ox2R\text{-}KO}$, U = 110.5, P = 0.897, Mann-Whitney test, n = 19 $DA^{Ox2R\text{-}CT}$, 12 $DA^{Ox2R\text{-}KO}$). (**k**) Representative heatmaps of a $DA^{Ox2R\text{-}CT}$ and a $DA^{Ox2R\text{-}KO}$ mouse during the habituation phase (left) and during social preference (right).

Analysis of social preference in $DA^{Ox2R\text{-}CT}$ and $DA^{Ox2R\text{-}KO}$ mice revealed that while control mice show normal social preference (**l**, time around social and empty enclosures for $DA^{Ox2R\text{-}CT}$, t (18) = 3.386, P = 0.003, paired t-test), and longer exploration bouts of the social than the inanimate target (**n**, average exploration bout duration $DA^{Ox2R\text{-}CT}$ mice: t (18) = 2.393, P = 0.028, paired t-test), $DA^{Ox2R\text{-}KO}$ mice neither exhibited social preference in % time spent around the juvenile mouse (**m**, paired comparison of time around the social vs empty enclosures for $DA^{Ox2R\text{-}KO}$, W = 30.00, P = 0.266, Wilcoxon test), nor manifested longer mean exploration bout duration for the social vs the inanimate target (**o**, paired comparison of average exploration bout duration for $DA^{Ox2R\text{-}KO}$, t (10) = 1.927, P = 0.083). Bar graphs show individual values and mean ± SEM. n = 19 $DA^{Ox2R\text{-}CT}$, 12 $DA^{Ox2R\text{-}KO}$.

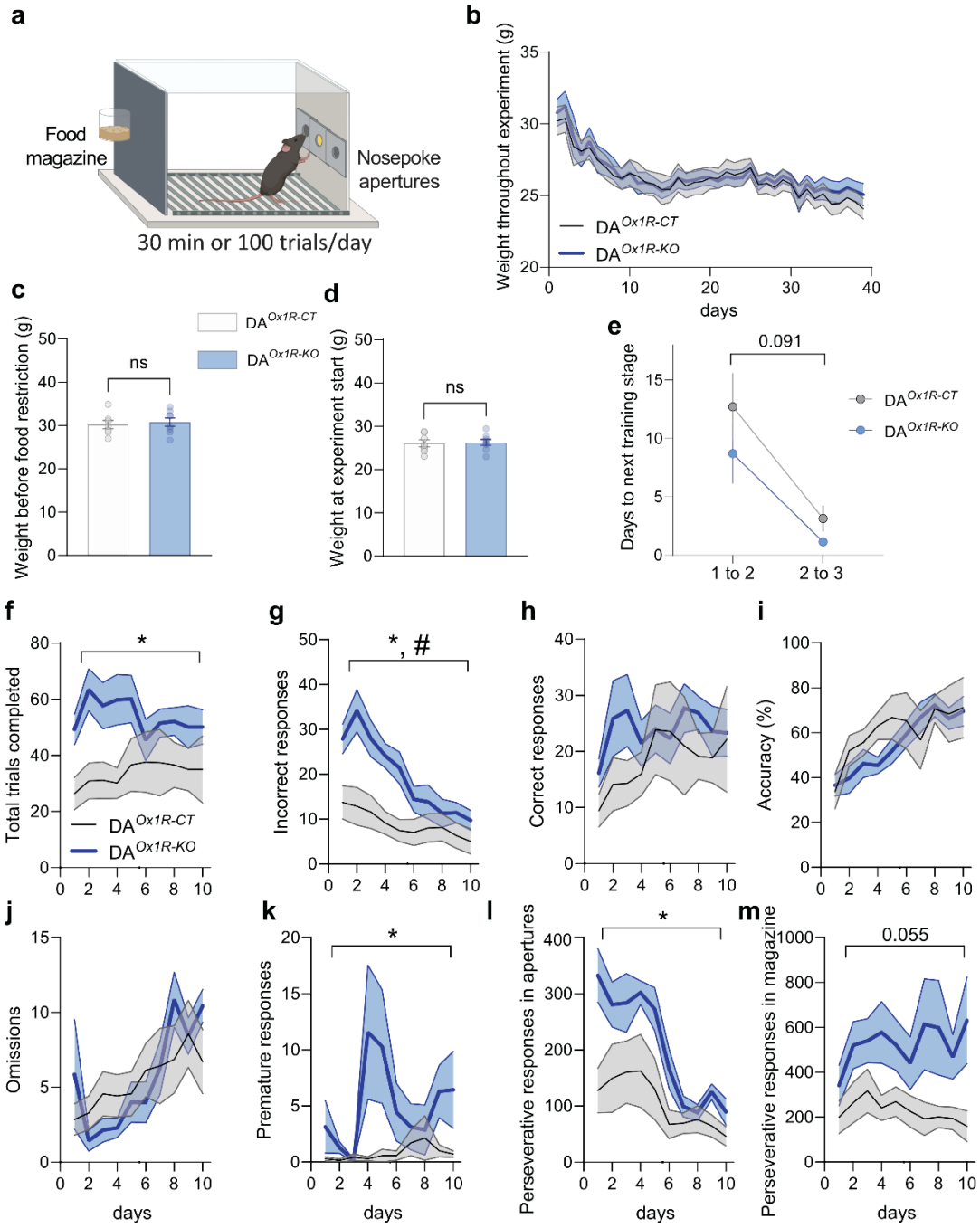

Fig. 4 Dopaminergic *Hcrtr1* ablation increases impulsive- and compulsive-like behaviors in a reward-driven operant conditioning task. Performance of DA$^{Ox1R\text{-}KO}$ (KO) and DA$^{Ox1R\text{-}CT}$ (CT) mice in the 3-choice serial reaction time task (3-CSRTT). (**a**) Schematic of the 3-CSRTT operant chamber. Three nosepoking apertures are located on the wall opposite the food magazine dispensing chocolate-flavored sucrose pellet awards. (**b**) A timeline of animal body weight throughout the 3-CSRTT procedure showed no difference between KO and CT mice (time: $F_{38,494} = 19.881$, $P < 0.001$; genotype: $F_{1,13} = 0.061$, $P = 0.808$; time × genotype: $F_{38,494} = 0.363$, $P = 1.000$, repeated measure 2-way ANOVA). (**c**) The initial body weight of mice before food restriction (t (13) = 0.417, $P = 0.683$, t-test), or (**d**) the body weight at the start of the 3-CSRTT procedure (t (13) = 0.200, $P = 0.844$, t-test) did not differ between KO and CT mice. $n = 7$ DA$^{Ox1R\text{-}CT}$, 8 DA$^{Ox1R\text{-}KO}$.

(**e**) DA$^{Ox1R\text{-}KO}$ mice showed a tendency to learn faster during the initial training days (training stages 1 to 3) relative to controls, as revealed by a comparison between the number of days to reach the next training stage in DA$^{Ox1R\text{-}KO}$ and DA$^{Ox1R\text{-}CT}$ mice (time: $F_{1,12}$ = 15.517, P = 0.002, genotype: $F_{1,12}$ = 1.827, P = 0.201, time × genotype: $F_{1,12}$ = 3.379, P = 0.091, repeated-measure 2-way ANOVA).

(**f**) DA$^{Ox1R\text{-}KO}$ completed a higher number of total trials compared to DA$^{Ox1R\text{-}CT}$ littermates [time: $F_{2.625,31.497}$ = 0.653, P = 0.567; genotype: $F_{1,12}$= 5.235, P = 0.041; time × genotype: $F_{2.625,31.497}$ = 1.183, P = 0.328, repeated-measure 2-way ANOVA], as well as (**g**) a higher number of incorrect responses during the 1st 10 training days (time: F (3.551, 42.611) = 14.670, P < 0.001; genotype: $F_{1,12}$ = 8.389, P = 0.013, time × genotype: F (3.551, 42.611) = 4.413, P = 0.006, repeated-measure 2-way ANOVA).

DA$^{Ox1R\text{-}KO}$ mice, however, did not differ from DA$^{Ox1R\text{-}CT}$ mice in (**h**) number of correct responses (time: $F_{1.977,23.719}$ = 1.614, P = 0.220, genotype: $F_{1,12}$ = 0.863, P = 0.371, time × genotype: $F_{1.977,23.719}$ = 0.762, P = 0.476, repeated-measure 2-way ANOVA), or (**i**) accuracy (time: $F_{2.372,28.461}$ = 8.731, P < 0.001, genotype: $F_{1,12}$ = 0.320, P = 0.582, time × genotype: $F_{2.372,28.461}$ = 1.258, P = 0.304, repeated measure 2-way ANOVA), or (**j**) number of omissions (time: $F_{2.630,31.563}$ = 5.033, P = 0.008; genotype: $F_{1,12}$ = 0.009, P = 0.928; time × genotype: $F_{2.630,31.563}$ = 1.380, P = 0.268, repeated-measure 2-way ANOVA) during the first 10 training days.

(**k**) DA$^{Ox1R\text{-}KO}$ mice exhibited a higher number of premature responses compared to DA$^{Ox1R\text{-}CT}$ mice during the 1st 10 training days (time: $F_{2.175,26.100}$ = 1.573, P = 0.226, genotype: $F_{1,12}$ = 5.775, P = 0.033, time × genotype: $F_{2.175,26.100}$ = 1.767, P = 0.189, repeated-measure 2-way ANOVA), (**l**) a higher number of repetitive nosepoking responses in any of the 3 apertures (time: $F_{3.456,41.468}$ = 13.310, P < 0.001, genotype: $F_{1,12}$ = 6.294, P = 0.027, time × genotype: $F_{3.456,41.468}$ = 2.478, P = 0.067, repeated-measure 2-way ANOVA), as well as (**m**) a trend towards a higher number of repetitive nosepoking responses in the food magazine (time: $F_{2.753,33.031}$ = 1.451, P = 0.247, genotype: $F_{1,12}$ = 4.501, P = 0.055, time × genotype: $F_{2.753,33.031}$ = 1.677, P = 0.194, repeated-measure 2-way ANOVA).

Bar graphs and timelines depict mean ± SEM. n = 7 DA$^{Ox1R\text{-}CT}$, 7 DA$^{Ox1R\text{-}KO}$. * denotes a significant genotype effect, and # a significant time × genotype effect, in repeated-measure 2-way ANOVA.

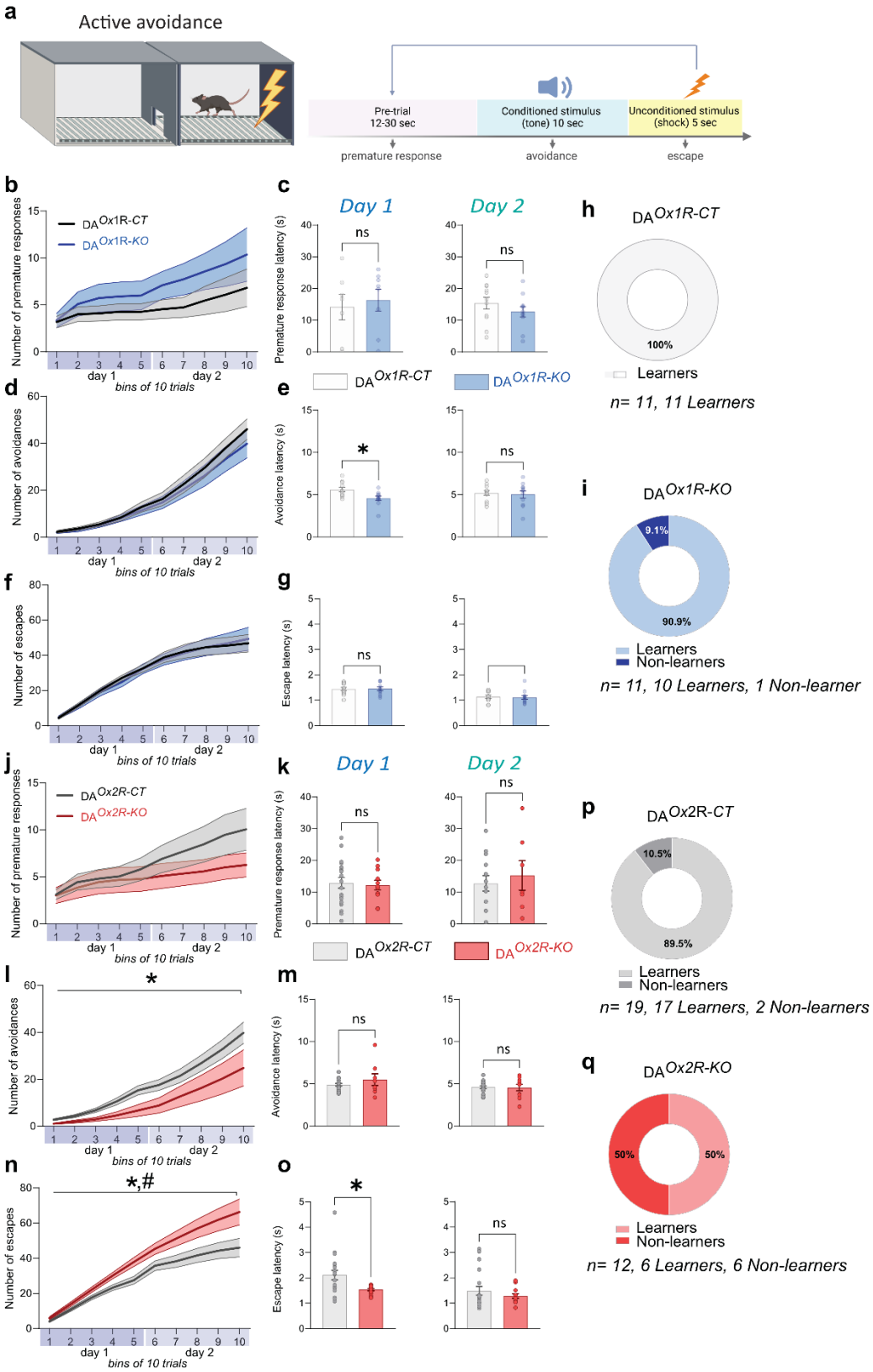

Fig. 5 Dopaminergic *Hcrtr2*-ablated mice show impaired aversion-driven instrumental learning in an active avoidance task. Performance of DA$^{Ox1R\text{-}KO}$ vs DA$^{Ox1R\text{-}CT}$ and DA$^{Ox2R\text{-}KO}$ vs DA$^{Ox2R\text{-}CT}$ mice in an active avoidance task. (**a**) Schematic of the active avoidance shuttle box and experimental design. An inter-chamber run during the pre-trial is a premature response, an inter-chamber run during the tone is an

avoidance response (indicative of successful learning), an inter-chamber run during the shock is an escape response.

(**b**) The number of premature responses did not differ between $DA^{Ox1R\text{-}CT}$ and $DA^{Ox1R\text{-}KO}$ mice across the 2 days of testing (time: $F_{1.233,24.668} = 7.511$, $P < 0.001$, genotype: $F_{1,20} = 1.374$, $P = 0.255$, time × genotype: $F_{1.233,24.668} = 0.878$, $P = 0.380$, repeated-measure 2-way ANOVA).

(**c**) Similar premature response latencies in $DA^{Ox1R\text{-}CT}$ and $DA^{Ox1R\text{-}KO}$ mice (Day 1, left: t (13) = 0.400, P = 0.695; Day 2, right: t (20) = 1.082, P = 0.292; t-tests).

(**d**) The number of avoidance responses did not differ between $DA^{Ox1R\text{-}CT}$ and $DA^{Ox1R\text{-}KO}$ mice across the 2 days of testing (time: $F_{1.126,\ 22.519} = 97.899$, $P < 0.001$; genotype: $F_{1,20} = 0.369$, $P = 0.550$; time × genotype: $F_{1.126,\ 22.519} = 0.502$, $P = 0.507$, repeated-measure 2-way ANOVA).

(**e**) $DA^{Ox1R\text{-}KO}$ mice showed shorter avoidance response latencies than $DA^{Ox1R\text{-}CT}$ in the 1st day of testing, indicating a faster avoiding response (Day 1, left: t (20) = 2.796, P = 0.011, Day 2, right: t (20) = 0.290, P = 0.775; t-tests).

(**f**) Number of escape responses did not differ between $DA^{Ox1R\text{-}CT}$ and $DA^{Ox1R\text{-}KO}$ mice across the 2 days of testing (time: $F_{1.156,23.113} = 102.588$, $P < 0.001$; genotype: $F_{1,20} = 0.003$, $P = 0.960$; time × genotype: $F_{1.156,23.113} = 0.200$, $P = 0.695$; repeated-measure 2-way ANOVA).

(**g**) Similar escape response latencies in $DA^{Ox1R\text{-}CT}$ and $DA^{Ox1R\text{-}KO}$ mice (Day 1, left: t (20) = 0.048, P = 0.962, and Day 2, right: U = 51.50, P = 0.573 t-test and Mann-Whitney test, respectively).

(**h**) and (**i**) Pie charts of learners vs non-learners in $DA^{Ox1R\text{-}CT}$ and $DA^{Ox1R\text{-}KO}$ show that both genotypes learn efficiently. n = 11 $DA^{Ox1R\text{-}CT}$, 11 $DA^{Ox1R\text{-}KO}$.

(**j**) The number of premature responses did not differ between $DA^{Ox2R\text{-}CT}$ and $DA^{Ox2R\text{-}KO}$ across the 2 days of testing (time: $F_{1.303,37.779} = 12.325$, $P < 0.001$, genotype: $F_{1,29} = 0.744$, $P = 0.396$, time × genotype: $F_{1.303,37.779} = 2.178$, $P = 0.143$, repeated-measure 2-way ANOVA)

(**k**) Similar premature response latencies in $DA^{Ox2R\text{-}CT}$ and $DA^{Ox2R\text{-}KO}$ mice (Day 1, left: t (28) = 0.290, P = 0.774; Day 2, right: t (18) = 0.528, P = 0.604; t-tests).

(**l**) $DA^{Ox2R\text{-}KO}$ mice show a decreased number of successful avoidance responses compared to $DA^{Ox2R\text{-}CT}$ mice across the 2 days of testing (time: $F_{1.146,33.242} = 46.938$, $P < 0.001$, genotype: $F_{1,29} = 4.507$, $P = 0.042$, time × genotype: $F_{1.146,33.242} = 2.084$, $P = 0.156$, repeated-measure 2-way ANOVA).

(**m**) Similar avoidance response latencies in $DA^{Ox2R\text{-}CT}$ and $DA^{Ox2R\text{-}KO}$ mice (Day 1, left: t (24) = 1.185, P = 0.248; Day 2, right: t (25) = 0.111, P = 0.912; t-tests).

(**n**) $DA^{Ox2R\text{-}KO}$ mice show an increased number of escapes (inter-chamber run after shock exposure) compared to $DA^{Ox2R\text{-}CT}$ mice, with both a genotype and a time x genotype significant effect (time: $F_{1.286,\ 37.284} = 126.005$, $P < 0.001$; genotype: $F_{1,29} = 6.354$, $P = 0.017$; time × genotype: $F_{1.286,\ 37.284} = 3.833$, $P = 0.048$, repeated-measure 2-way ANOVA).

(**o**) $DA^{Ox2R\text{-}KO}$ mice nevertheless show shorter escape response latencies than $DA^{Ox2R\text{-}CT}$mice in the 1st day of testing, suggesting that they are sensitive to the electric shock (Day 1, left: U = 62, P = 0.035; Day 2, right: U = 113, P = 0.984; Mann-Whitney tests).

(**p**) and (**q**) Pie charts of learners *vs* non-learners in $DA^{Ox2R\text{-}CT}$ and $DA^{Ox2R\text{-}KO}$ mice highlight the markedly reduced learning efficiency observed among $DA^{Ox2R\text{-}KO}$ mice. Bar graphs and timelines depict mean ± SEM. n = 19 $DA^{Ox2R\text{-}CT}$, 12 $DA^{Ox2R\text{-}KO}$.

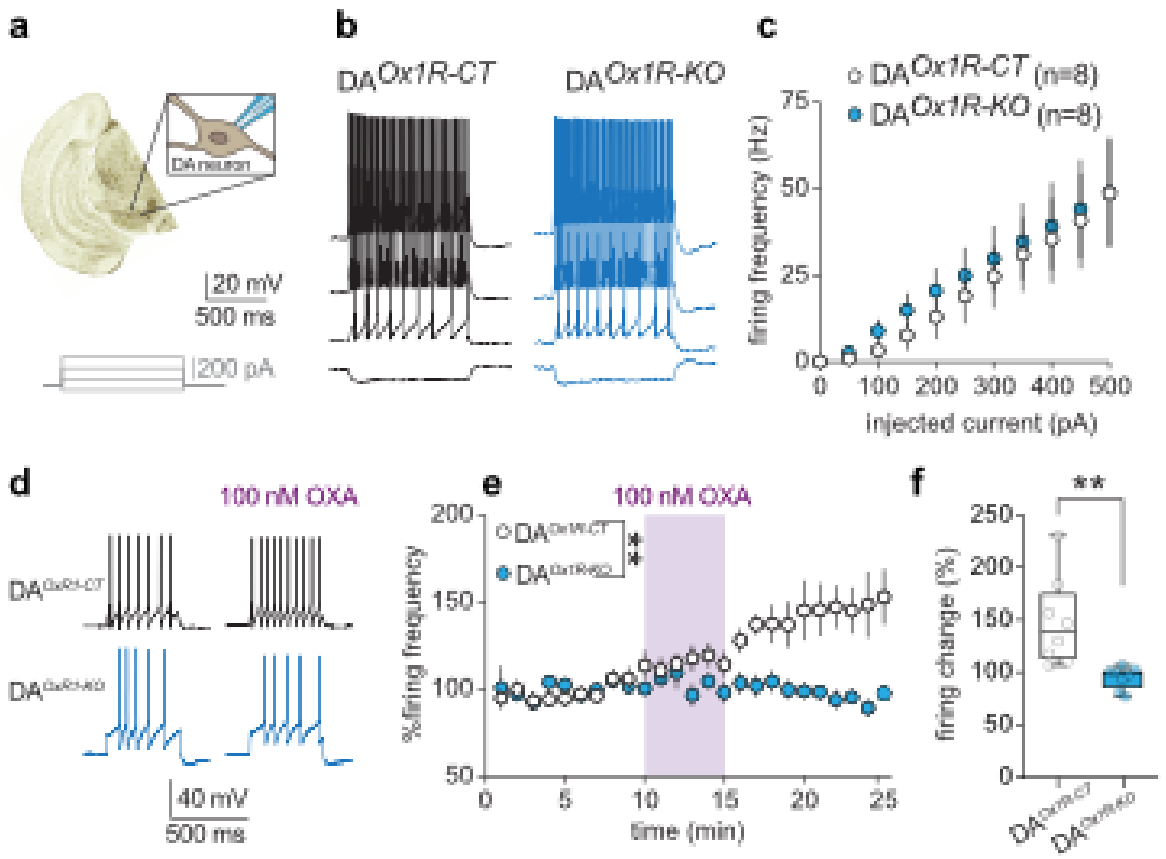

Fig. 6 OXA enhances excitability of DA^{VTA} neurons from control mice but not DA$^{Ox1R\text{-}KO}$ mice. (**a**) Scheme of *ex vivo* whole-cell patch-clamp recordings from DA neurons in VTA slices from DA$^{Ox1R\text{-}CT}$ and DA$^{Ox1R\text{-}KO}$ mice. (**b**) Representative traces of neuronal firing elicited by increasing somatic current injections. (**c**) Frequency-current relationship of action potential discharges shows no difference between CT and KO mice (2-way ANOVA for effect genotype $F_{1,14}$ = 0.1426; P = 0.711). (**d**) Examples of neuronal firing elicited in response to a depolarizing step prior to and after bath-application of OXA (100 nM) in DA neurons from DA$^{Ox1R\text{-}CT}$ and DA$^{Ox1R\text{-}KO}$ mice. (**e**) Mean firing frequency values normalized to the first 10 min (n=8 cells per genotype). OXA increased firing in DA$^{Ox1R\text{-}CT}$ but not in DA$^{Ox1R\text{-}KO}$ mice (2-way ANOVA for effect genotype $F_{1,14}$ = 10.45; P = 0.006; genotype × treatment interaction $F_{24,334}$ = 5.772; P <0.001). (**f**) Average OXA-induced change in neuronal firing in DA$^{Ox1R\text{-}CT}$ and DA$^{Ox1R\text{-}KO}$ mice (t (7.87) = 3.419; P = 0.009, t-test). Bar graphs show individual values and mean ± SEM. Timelines show mean ± SEM.

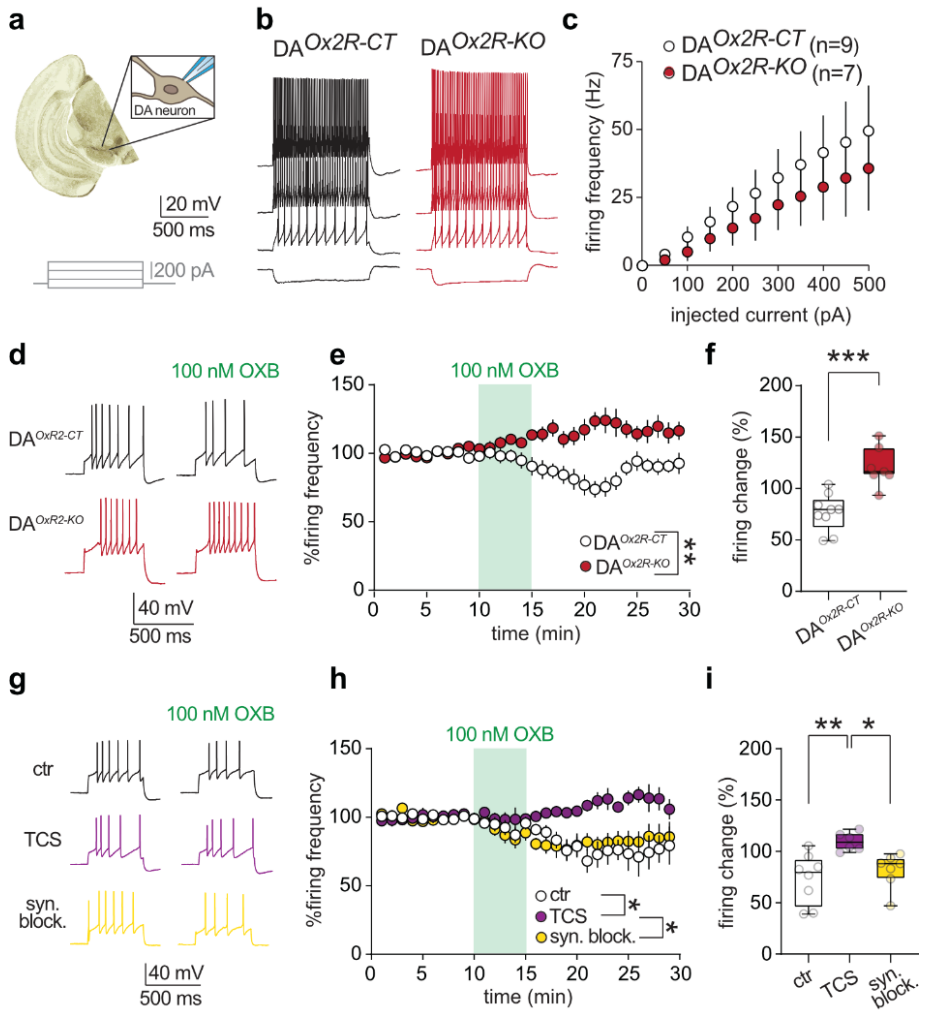

Fig. 7 OXB decreases excitability of DA^{VTA} neurons from control mice but not DA$^{Ox2R\text{-}KO}$ mice.

(**a**) Scheme of *ex vivo* patch-clamp recordings from DA neurons of DA$^{Ox2R\text{-}CT}$ and DA$^{Ox2R\text{-}KO}$ mice. (**b**) Representative traces of neuronal firing elicited by increasing somatic current injections. (**c**) Frequency-current relationship of action potential discharges shows no statistical difference between CT and KO mice (2-way ANOVA for effect genotype $F_{1,14} = 0.457$; $P = 0.510$). (**d**) Examples of neuronal firing elicited in response to a depolarizing step prior to and after bath-application of OXB (100 nM) in DA neurons from DA$^{Ox2R\text{-}CT}$ and DA$^{Ox2R\text{-}KO}$ mice. (**e**) Mean firing frequency values normalized to the first 10 min (n=9:7 cells, CT:KO). OXB transiently decreased firing in DA$^{Ox2R\text{-}CT}$ (paired *t* test; $t_8 = 3.546$; $P = 0.008$), but not DA$^{Ox2R\text{-}KO}$ mice, which showed instead a tendency towards increased firing ($t_6 = 2.132$; $P = 0.077$, paired t-test). 2-way ANOVA revealed a genotype effect ($F_{1,14} = 14.87$; $P = 0.002$) and a significant genotype × treatment interaction ($F_{28,383} = 6.484$; $P < 0.001$). (**f**) Average OXB-induced change in neuronal firing in DA$^{Ox2R\text{-}CT}$ and DA$^{Ox2R\text{-}KO}$ mice ($t_{12.72} = 4.729$; $P < 0.001$, *t*-test). (**g**) Representative examples of neuronal firing elicited by a depolarizing step before and after bath application of OXB (100 nM) in DA neurons from VTA slices prepared from C57BL/6J mice under three conditions: control (ctr, without blockers), in the presence of the OX_2R antagonist TCS-OX2-29 (10 µM), and in the presence of synaptic blockers (syn. block.; 10 µM DNQX, 50 µM D,L-APV, 100 µM picrotoxin). (**h**) Mean firing frequency normalized to the first 10 min for each experimental group (n = 8, 6, 7, respectively). OXB decreased firing in the

control condition (W = -32; P = 0.023, Wilcoxon test) and in the presence of synaptic blockers (t (6) = 2.634; P = 0.039, paired t-test), but not when OX_2R receptors were blocked (t_6 = 1.662; P = 0.148, paired t-test). A mixed-effects analysis revealed a significant effect of OXB ($F_{30, 570}$ = 2.787; P < 0.001) and a significant effect of the blockers ($F_{2,18}$ = 6.433; P < 0.01). (**i**) Average OXB-induced change in neuronal firing across the three groups ($F_{2,18}$ = 6.815; P = 0.006, one-way ANOVA). Asterisks indicate statistical significance as determined by Holm-Šídák's multiple comparisons test (*P<0.05; **P<0.01).

Supplementary Information

Divergent modulation of dopaminergic neurons by hypocretin/orexin receptors-1 and -2 shapes dopaminergic cell activity and socio-emotional behavior

Stamatina Tzanoulinou[1], Simone Astori[2], Laura Clara Grandi[3], Francesca Gullo[3], Richie Kalusivikako[1], Simran Rai[1], Mehdi Tafti[1], Andrea Becchetti[3], and Anne Vassalli[1] ✉

[1] *Department of Biomedical Sciences, University of Lausanne, Lausanne, Switzerland.*
[2] *Laboratory of Behavioral Genetics, EPFL, Switzerland.*
[3] *Department of Biotechnology and Biosciences, University of Milano-Bicocca, Milano, Italy.*

✉Corresponding author: anne.vassalli@unil.ch

Supplementary Information consists of:

Figures S1-S3

Table S1

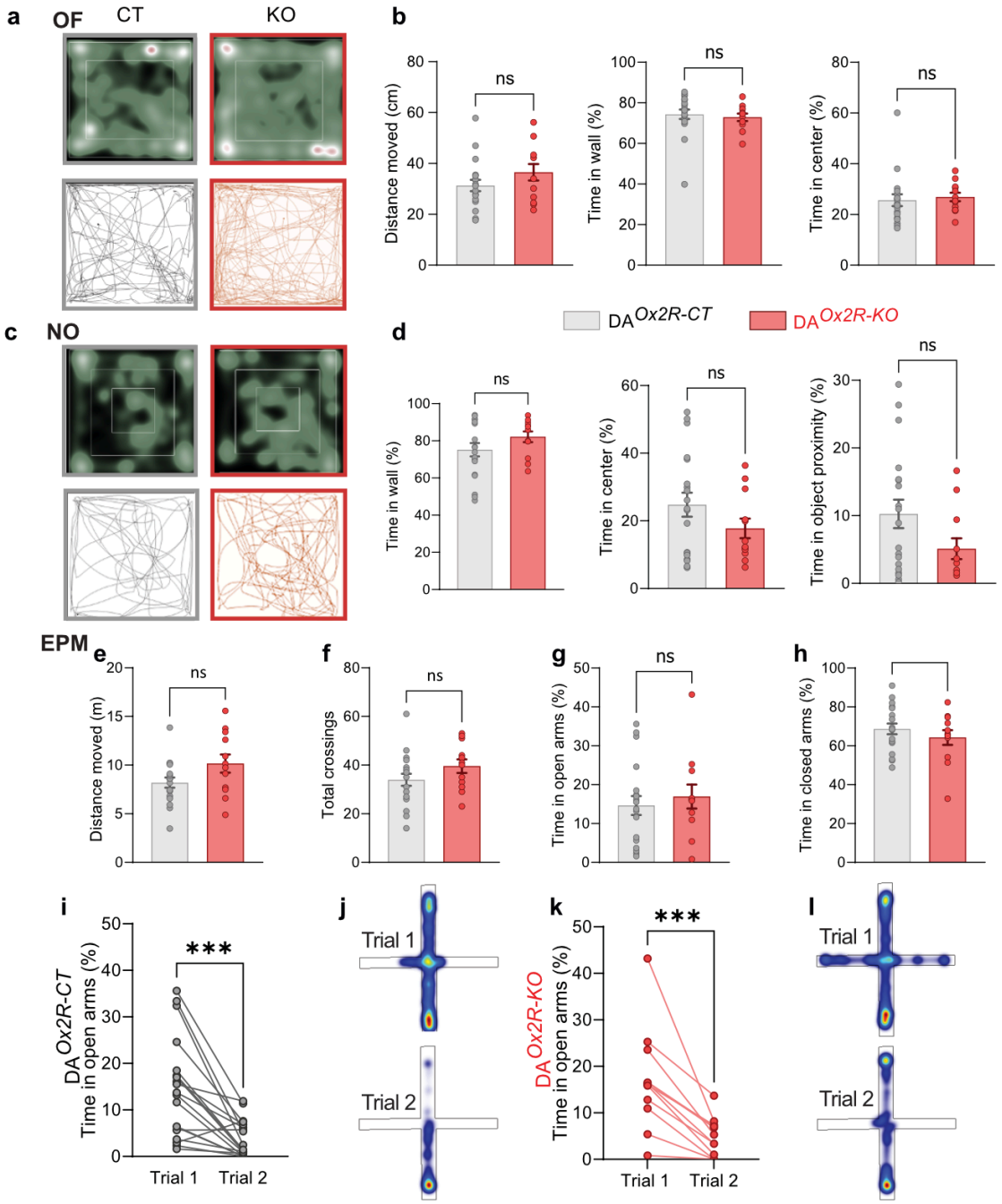

Fig. S1 Dopaminergic *Hcrtr2*-ablated mice show normal explorative behavior, reactivity to novelty, and responses in the elevated plus maze.

Behavioral profiling of DA$^{Ox2R\text{-}KO}$ and DA$^{Ox2R\text{-}CT}$ mice in the open field (OF), reactivity to novel object (NO) and elevated plus maze (EPM) tests. (**a**) Example heat maps (top) and trail maps (bottom) from DA$^{Ox2R\text{-}CT}$ (left) and DA$^{Ox2R\text{-}KO}$ (right) in the open field arena during 10-min free exploration.

(**b**) (Left) distance moved comparison between DA$^{Ox2R\text{-}CT}$ and DA$^{Ox2R\text{-}KO}$ in the open field for 10 min, t (29) =1.366, P = 0.1883, t-test, middle: comparison between DA$^{Ox2R\text{-}CT}$ and DA$^{Ox2R\text{-}KO}$ for the time in the wall zone for 10 min, U = 85, P = 0.252, Mann-Whitney test, right: time in the center zone for 10 min in DA$^{Ox2R\text{-}CT}$ and DA$^{Ox2R\text{-}KO}$ (U = 86, P = 0.269, Mann-Whitney test).

(**c**) Example heat maps (Top) and trail maps (Bottom) from $DA^{Ox2R\text{-}CT}$ (Left) and $DA^{Ox2R\text{-}KO}$ (Right) in the arena for 5 min after placing a novel object.
(**d**) (Left) comparison between $DA^{Ox2R\text{-}CT}$ and $DA^{Ox2R\text{-}KO}$ for the time in the wall zone during the reactivity to the novel object phase, t (29) = 1.383, P = 0.177, t-test, middle: comparison between $DA^{Ox2R\text{-}CT}$ and $DA^{Ox2R\text{-}KO}$ for the time in the center zone for 5 min during the reactivity to the novel object phase, t (29) = 1.389, P = 0.175, t-test, right: comparison between $DA^{Ox2R\text{-}CT}$ and $DA^{Ox2R\text{-}KO}$ for the time in the center zone around the novel object, U = 77, P = 0.138, Mann-Whitney test.
(**e**) Total distance traveled by $DA^{Ox2R\text{-}CT}$ and $DA^{Ox2R\text{-}KO}$ mice in the EPM, t (29) = 1.980, P = 0.057, t-test.
(**f**) Number of total inter-zone crossings in $DA^{Ox2R\text{-}CT}$ and $DA^{Ox2R\text{-}KO}$ mice, t (29) = 1.476, P = 0.151, t-test.
(**g**) Time in the open arms of the EPM by $DA^{Ox2R\text{-}CT}$ and $DA^{Ox2R\text{-}KO}$ mice (t (29) = 0.5586, P = 0.562, t-test.
(**h**) Time in the closed arms of the EPM by $DA^{Ox2R\text{-}CT}$ and $DA^{Ox2R\text{-}KO}$, t (29) = 0.975, P = 0.337, t-test.
(**i**) Comparison of the time in open arms between trial 1 and trial 2 for $DA^{Ox2R\text{-}CT}$, and example heatmaps for trial 1 and trial 2, W = -176, P < 0.001, Wilcoxon test.
(**k**) Comparison of the time in open arms between trial 1 and trial 2 for $DA^{Ox2R\text{-}KO}$, and example heatmaps for trial 1 and trial 2, t (12) = 5.054, P < 0.001, paired t-test.
Bar graphs show individual values and mean ± SEM. n = 19 $DA^{Ox2R\text{-}CT}$, 12 $DA^{Ox2R\text{-}KO}$.

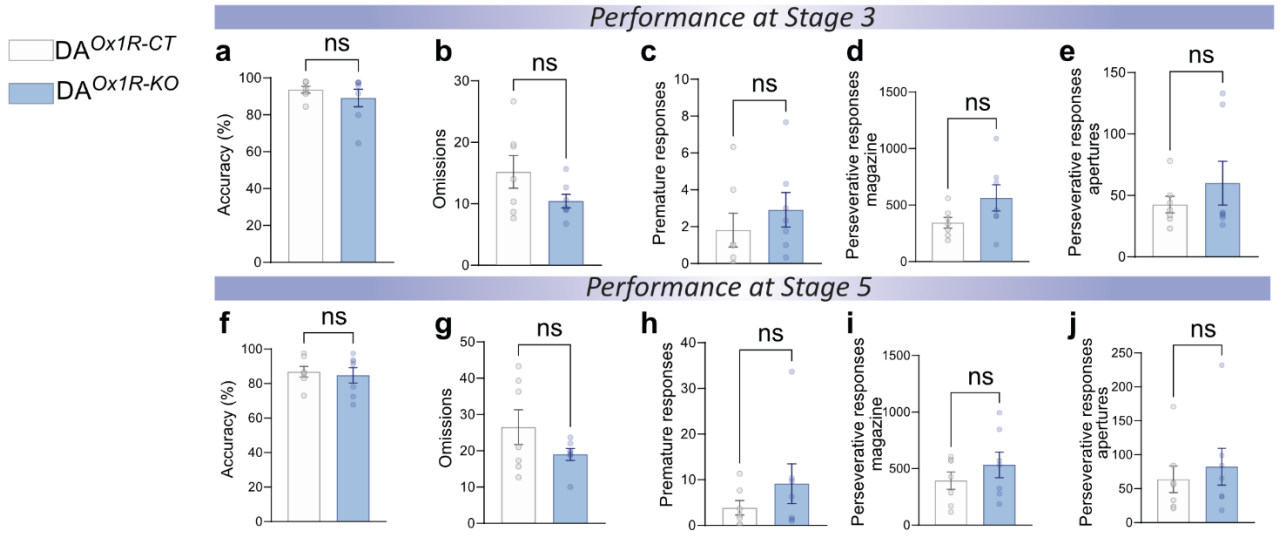

Fig. S2 Similar performance of DA$^{Ox1R\text{-}KO}$ and DA$^{Ox1R\text{-}CT}$ mice in the three-choice serial reaction time task (3-CSRTT) in stage 3 (a-e) and stage 5 (f-j) contingencies.

(**a**) Accuracy score at stage 3 in DA$^{Ox1R\text{-}CT}$ and DA$^{Ox1R\text{-}KO}$ mice (U = 19, P = 0.535, Mann-Whitney test).

(**b**) Omission rate at stage 3 in DA$^{Ox1R\text{-}CT}$ and DA$^{Ox1R\text{-}KO}$ mice (t (12) = 1.659, P = 0.123, t-test).

(**c**) Premature responses at stage 3 in DA$^{Ox1R\text{-}CT}$ and DA$^{Ox1R\text{-}KO}$ mice f(U = 14.50, P = 0.223, Mann-Whitney test)

(**d**) Rate of perseverative responding in the food magazine at stage 3 in DA$^{Ox1R\text{-}CT}$ and DA$^{Ox1R\text{-}KO}$ mice (t (12) = 1.756, P = 0.105, t-test).

(**e**) Rate of perseverative responding in nosepoking apertures at stage 3 in DA$^{Ox1R\text{-}CT}$ and DA$^{Ox1R\text{-}KO}$ mice (U = 23.50, P = 0.929, Mann-Whitney test).

(**f**) Accuracy scores at stage 5 of DA$^{Ox1R\text{-}CT}$ and DA$^{Ox1R\text{-}KO}$ mice (t *(12)* = 0.383, P = 0.709, t-test).

(**g**) Omission responding rate at stage 5 inDA$^{Ox1R\text{-}CT}$ and DA$^{Ox1R\text{-}KO}$ mice (t (12) = 1.483, P = 0.164, t-test.

(**h**) Rate of premature responding at stage 5 in DA$^{Ox1R\text{-}CT}$ and DA$^{Ox1R\text{-}KO}$ mice (U = 18.50, P = 0.476, Mann-Whitney test).

(**i**) Rate of perseverative responding in the food magazine at stage 5 in DA$^{Ox1R\text{-}CT}$ and DA$^{Ox1R\text{-}KO}$ mice (t (12) = 1.015, P = 0.330, t-test).

(**j**) Rate of perseverative responding in nosepoking apertures at stage 5 in DA$^{Ox1R\text{-}CT}$ and DA$^{Ox1R\text{-}KO}$ mice (U = 19.50, P = 0.558, Mann-Whitney test).

Bar graphs show individual values as mean ± SEM. n = 7 DA$^{Ox1R\text{-}CT}$, 7 DA$^{Ox1R\text{-}KO}$.

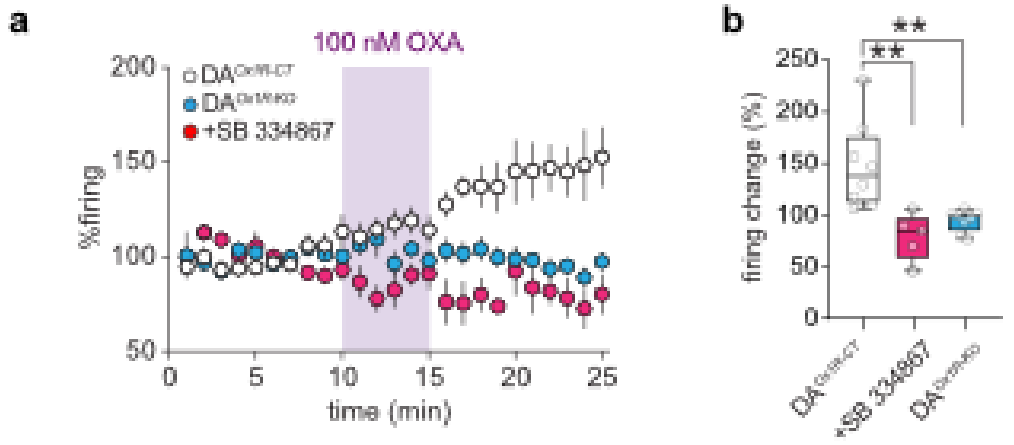

Fig. S3 Enhancement of DA^{VTA} neuronal excitability by OXA is OX_1R-dependent.
(**a**) Mean values of firing frequency elicited in response to a depolarizing step prior to and after bath-application of OXA (100 nM) in DA neurons from $DA^{Ox1R\text{-}CT}$ mice in control condition (n=8) and in the presence of the OX_1R antagonist SB-334867 (1 µM; n=5), and in $DA^{Ox1R\text{-}KO}$ mice (n=8). (**b**) Average OXA-induced change in neuronal firing in $DA^{Ox1R\text{-}CT}$ mice. This effect was abolished by OX_1R blockade and in $DA^{Ox1R\text{-}KO}$ mice ($F_{2,18}$ = 10.42; P<0.01, one-way ANOVA).
Note that data shown in (a-b) from $DA^{Ox1R\text{-}CT}$ mice in control condition are retaken from Fig. 6 e-f.
Bar graphs show individual values and mean ± SEM. Timelines show mean ± SEM.

Training stage	Stimulus duration (s)	ITI (s)	LHD (s)	Criterion to move to next stage
1	30	2	30	≥ 30 Correct trials
2	15	2	15	≥ 30 Correct trials
3	10	5	10	≥ 50 Correct trials
4	7	5	7	≥ 50 Correct trials > 70% Accuracy
5	5	5	5	≥ 50 Correct trials > 70% Accuracy < 20% Omissions
6	4	5	4	≥ 50 Correct trials > 70% Accuracy < 20% Omissions
7	3	5	3	≥ 50 Correct trials > 70% Accuracy < 20% Omissions
8	2	5	2	≥ 50 Correct trials > 70% Accuracy < 20% Omissions
9	1.5	5	1.5	≥ 50 Correct trials > 70% Accuracy < 20% Omissions
10	1.2	5	1.2	≥ 50 Correct trials > 70% Accuracy < 20% Omissions

Table S1. Criteria used to define the test contingencies of the 10 different stages of gradually increasing difficulties used in the 3-choice serial reaction time task test (3-CSRTT) described in Fig. 4.
ITI, inter-trial-interval, LHD, limited-hold period.